DESIGN OF COLUMNS SUBJECT TO LOCALISED FIRES

SCI Steel Knowledge

Ulster University

SCI (The Steel Construction Institute) is the leading, independent provider of technical expertise and disseminator of best practice to the steel construction sector. We work in partnership with clients, members and industry peers to help build businesses and provide competitive advantage through the commercial application of our knowledge. We are committed to offering and promoting sustainable and environmentally responsible solutions.

Our service spans the following areas:

Membership
Individual & corporate membership

Advice
Members advisory service

Information
Publications
Education
Events & training

Consultancy
Development
Product development
Engineering support
Sustainability

Assessment
SCI Assessment

Specification
Websites
Engineering software

Publication Number: **SCI P423**

ISBN

Published by:

SCI, Silwood Park, Ascot,
Berkshire. SL5 7QN UK

T: +44 (0)1344 636525
F: +44 (0)1344 636570
E: reception@steel-sci.com

www.steel-sci.com

To report any errors, contact:
publications@steel-sci.com

Front cover photo:
A localised fire test carried out at the University of Ulster.

British Library Cataloguing-in-Publication Data.
A catalogue record for this book is available from the British Library.

Photo credits:
Unless otherwise noted, the photographs were provided by members of the LOCAFI consortium.

This design guide was written and confirmed by Phil Francis, Nancy Baddoo, Francois Hanus, Christopher Thauvoye, Ali Nadjai.

FOREWORD

This publication has been prepared as part of the European Union's Research Fund for Coal and Steel Project *Temperature assessment of a vertical steel member subjected to localised fire – Valorisation (LOCAFI-plus)* (contract 754072).

The organisations who participated in the LOCAFI-plus project were:

Arcelormittal Belval & Differdange SA
Luxembourg

Centre Technique Industriel de la Construction Métallique
France

Universitatea Politehnica Timisoara
Romania

Universite de Liège
Belgium

University Of Ulster
UK

Universita Degli Studi Di Trento
Italy

Ceske Vysoke Uceni Technicke V Praze
Czech Republic

Stichting Bouwen met Staal
The Netherlands

Universidade de Aveiro
Portugal

Bauforumstahl ev
Germany

Tallinna Tehnikaulikool
Estonia

Univerza V Ljubljani
Slovenia

Instytut Techniki Budowlanej
Poland

Universitat Politecnica de Valencia
Spain

Technicka Univerzita V Kosiciach
Slovakia

Staalinfocentrum – Infosteel
Belgium

Miskolci Egyetem
Hungary

Tampere University of Technology
Finland

The Steel Construction Institute
UK

SP Sveriges Tekniska Forskningsinstitut AB
Sweden

The following people made a significant contribution to the preparation of this publication:

- Phil Francis, SCI
- Nancy Baddoo, SCI
- Francois Hanus, ArcelorMittal
- Christophe Thauvoye, CTICM

The contour plots were developed by CTICM.

The financial support from the Research Fund for Coal and Steel is gratefully acknowledged.

Contents

1 INTRODUCTION

1.1 Scope of this design guide

This design guide presents a method for determining the temperature of a column subject to a localised fire. The approach is aligned to the Eurocodes. Guidance on how to determine the resistance of a steel column when subject to elevated temperatures is also given. The use of this performance-based approach for assessing structural fire resistance will usually lead to a reduction in the cost of fire protection compared to that required by a prescriptive approach.

The guide includes the following contents:

- A general introduction to fire engineering, including the selection of modelling scenarios and calculation techniques.
- Specific guidance on localised fire design, including a summary of the investigative work performed as part of the European research project LOCAFI.
- A new design model for localised fires.
- A description of the design tools available for modelling localised fires, ranging from simplified analysis using contour plots, to sophisticated finite element models.
- A summary of the Eurocode 3 design resistance model for steel columns in fire, which may be used with the temperature analysis model to give a column resistance.
- Design examples, demonstrating the use of the model in realistic design scenarios.

1.2 The Eurocodes

The Eurocodes are a series of 10 European Standards, EN 1990 - EN 1999, providing a common approach to the design of buildings and other civil engineering works and construction products. When considering the fire resistance of a steel or composite steel and concrete member, the following Eurocodes are relevant:

- EN 1990 Eurocode 0. Basis of structural design[1]
- EN 1991-1-2 Eurocode 1. Actions on Structures. Actions on Structures exposed to fire[2]
- EN 1993-1-2 Eurocode 3. Design of steel structures. General rules. Structural fire design[3]
- EN 1994-1-2 Eurocode 4. Design of composite steel and concrete structures. General rules. Structural fire design[4]

Each of these Eurocodes is accompanied by a National Annex which, where appropriate, will:

- Specify the value of a factor (called a Nationally Determined Parameter),
- Specify which design method to use,
- State whether an informative annex may be used.

In addition, the National Annex may give references to publications that contain non-contradictory complimentary information (NCCI) that will assist the designer. The guidance given in a National Annex applies to structures that are to be constructed within that country. National Annexes are likely to differ between countries within Europe.

1.3 National regulations on performance-based fire engineering

Understanding of the advantages and limitations of performance-based fire engineering has improved in recent years. However, there is considerable variation across Europe in the national building control regulations relating to fire safety. For this reason, it is essential that the designer is aware of the relevant legislation in the country in which the structure will be situated, and has engaged with the relevant checking and approval authority at the appropriate stage in the design.

To assist with this, guidance on the steps required to gain approval for using performance-based fire engineering methods in different European countries is available here:http://research.bauforumstahl.com/.

2 INTRODUCTION TO FIRE ENGINEERING

Fire represents a severe threat to human life. It is essential that buildings are designed and constructed so that, in the event of a fire, their stability will be maintained for a long enough period to allow both the evacuation of the occupants and the initiation of fire containment measures. Fire engineering is the application of scientific principles to the design of structures to ensure the safety of the occupants in all reasonable scenarios.

Fire engineering encompasses a wide range of issues including:

- Minimising the risk of fire starting in the first place,
- Containment of the fire at its ignition point i.e. stopping the fire spreading to other parts of the building or other structures,
- Provision of firefighting measures e.g. sprinklers,
- Provision of fire protection to the structure, such that collapse is prevented,
- Understanding of human reaction to fire e.g. response to alarms, ability to find safe evacuation routes etc.

Provision of measures to minimise the impact of the fire can form a significant portion of the cost of the structure. Over-specification of fire protection measures can lead to uneconomic structures. A balanced solution is required which provides adequate protection against the design fire scenarios at minimum cost to the client.

For more information on fire engineering, the following publications are recommended[5,6,7,8].

This design guide gives a method for estimating the temperature rise in a column subject to a localised fire. Once the temperature is known, the resistance of the column can be determined. As explained in Section 2.2, this performance-based fire engineering approach can lead to significant reduction in fire protection, and hence cost, compared to that required from a prescriptive approach.

2.1 Design against collapse and provision of fire protection

Preventing collapse is one of the key goals in the fire engineering process. Collapse represents a sudden and catastrophic loss of stability in the structure, and will usually result in the death of any occupants present in the building at the time, whether they are building users or firefighting personnel.

Collapse of a building is generally prevented by protecting the structural elements. Fire protection usually takes one of two forms, non-reactive (e.g. boards and sprays) and reactive (intumescent coatings). Boarded fire protection provides insulation from fire through the use of highly insulative cementitious particle boards with high density and low thermal conductivity. Cementitious particles may also be applied by spray.

Intumescent coatings are paint-like materials which are inert at low temperatures but provide insulation as a result of a complex chemical reaction at temperatures typically of about 200-250°C. At these temperatures the properties of steel will not

be affected. As a result of this reaction they swell and provide an expanded layer of low conductivity char.

The insulating effect of a board, sprayed or painted system tends to be proportional to the thickness of material provided. It is therefore conservative to provide more fire protection than is required. However, this increases the cost. It is sometimes more economic to specify a larger unprotected member than a smaller protected member, since the cost of fire protection is eliminated.

In many cases it can be proven that the structure is capable of remaining functional without the provision of fire protection.

Selection of the thickness of fire protection material requires the following factors to be considered:

(a) The severity of the fire, and the anticipated temperature rise in the member,

(b) The properties of the fire protection material,

(c) The temperature to which the protected member can be allowed to reach before collapse occurs, termed the 'critical temperature'.

Rules for determining the resistance of the structure in fire are given in the Eurocodes (Section 5).

2.2 Design to the Eurocodes

A complete fire design requires the use of a number of the Eurocodes in combination. EN 1991-1-2, clause 2.1 sets out four main steps in a structural fire design analysis:

- Selection of relevant design fire scenarios,
- Determination of the corresponding design fires,
- Calculation of temperature evolution within the structural members,
- Calculation of the mechanical behaviour of the structure exposed to fire, using EN 1993-1-2 for steel structures.

2.2.1 Design fire scenarios

EN 1991-1-2, clause 2.2 describes the process of selecting a fire design scenario.

A prescriptive approach to fire engineering often involves the use of the standard temperature-time curve. This is one of the three nominal temperature-time curves given by the Eurocode and is intended to model the temperature rise in a fully developed compartment fire (Section 2.2.2 of this document).

Most office building structures are of a reasonably standard size and shape and a prescriptive approach to fire engineering is considered sufficient. The thickness of fire protection is determined assuming engulfment in a fire which follows the standard temperature-time curve, and depends on the dimensions of the section and the fire resistance requirement.

However, for certain types of structures such as airports and other large open buildings, application of the standard temperature-time curve is not always appropriate; design based on the properties of the actual fire will produce more accurate, and usually more economic, designs. This is known as a performance-based fire engineering approach and requires an understanding of both the material that may cause the fire and the size and ventilation characteristics of the compartment in which the fire is contained. Selection of the appropriate design fire

scenario and modelling techniques are important to ensure the adequacy of the design.

2.2.2 Compartment fire

A fully developed compartment fire occurs when all of the combustible material in a room is simultaneously ignited, which occurs at the point of 'flashover'. It can be reasonably assumed that the temperature within the compartment is uniform throughout the compartment. Figure 2.1 shows an example of a compartment fire.

Photo credit: Czech Technical University in Prague

Figure 2.1 A compartment fire

2.2.2.1 Standard temperature-time curve

The variation of the temperature inside the compartment with time can be described using the standard temperature-time curve given in EN 1991-1-2. The curve is a reference curve only, and is not intended to represent any specific fire scenario. For most situations it is found to be very conservative compared to recorded data. No allowance is made for loss of temperature as the combustible material is used up.

The standard temperature-time curve is expressed as:

$$\theta_g = 20 + 345 \log(8t + 1) \qquad (2.1)$$

Where:

θ_g is the gas temperature in the fire compartment

t is the time, measured in minutes

Figure 2.2 shows the temperature vs. time relationship defined by the standard fire curve.

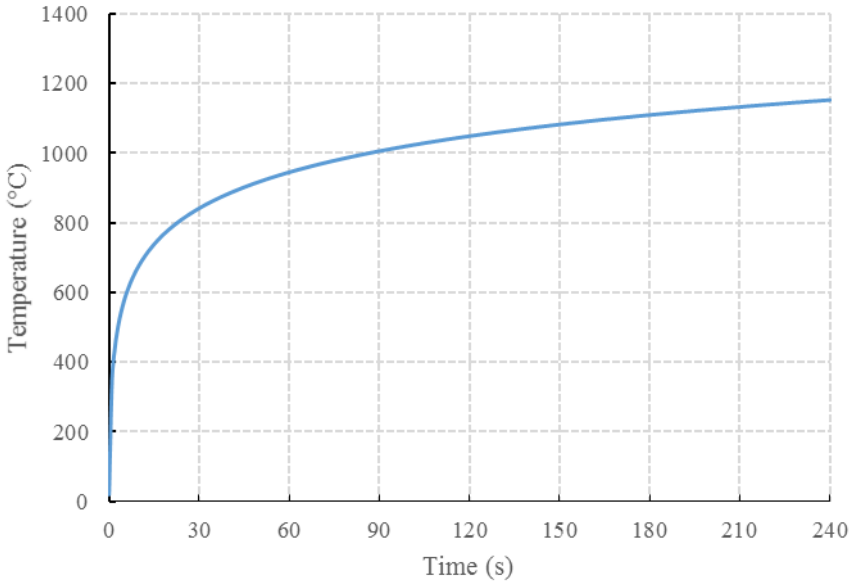

Figure 2.2 Standard temperature-time curve

2.2.2.2 Other fire design approaches

Use of the standard temperature-time curve tends to lead to fire protection provision that is economically acceptable for most ordinary structures. However, some designs may warrant a more detailed and realistic analysis, which may result in reduced design temperatures.

The severity of a compartment fire is influenced by several factors, including:

- Combustible material type, density and distribution,
- Compartment size and geometry
- Ventilation and air-flow conditions

The temperature-time curve for the compartment can alternatively be determined from natural fire models, such as the parametric temperature-time model (given in EN 1991-1-2 Annex A), a zone model (given in EN 1991-1-2 Annex D or a computational fluid dynamics (CFD) model (see 2.2.4 for more details). These models allow the gas temperature in the compartment to be calculated as a function of compartment geometry, ventilation conditions, thermal properties of the compartment boundaries, the fire growth rate and fire load density. It should be noted that use of EN 1991-1-2 Annex A is not allowed by the National Annexes of a number of countries.

2.2.3 Localised (non-compartment) fires

The compartment fire scenario assumes that the temperature of the compartment rises uniformly. For compartments that are reasonably small and where the fire load is uniformly distributed, this is usually reasonably realistic. However, as the size of the compartment increases or if the fire load is located in a relatively small area, this assumption tends to become increasingly conservative. In these cases, an approach which takes into account the variation in temperature with location can produce significantly less conservative results, though the analysis required to produce the temperature profile is considerably more complex.

Analysis using localised fire models is the focus of Section 3.

2.2.4 Computational fluid dynamics (CFD)

A fire presents a complex mix of physical phenomena which means that simple approaches cannot always be used to accurately reproduce the temperatures associated with a fire design scenario. In these cases, sophisticated software models based on CFD may provide the best available representation of the fire to the designer. CFD can be used to model all conceivable fire scenarios, including fully developed fires, localised fires, fires outside buildings etc.

Reproduction of the physical phenomena required to accurately reproduce a fire is extremely difficult. Turbulence in particular cannot be computed with full accuracy at any scale; instead, a number of semi-empirical models are generally used to approximate the overall effects. The range of potential models is large and careful choice of the most appropriate model for the given situation is required. For these reasons, CFD is typically undertaken only by experts.

A useful introduction to CFD techniques for modelling fires can be found in *Guide to the advanced fire safety engineering of structures*[9].

3 LOCALISED FIRES

As first discussed in Section 2, prescriptive rules for fire design typically assume a fully engulfed compartment, with a uniform temperature throughout the space. Such an assumption tends to be particularly onerous for large compartments. Performance-based fire engineering allows the user to take into account the real behaviour of fires, which can often be highly localised. In these cases, an understanding of how localised fires behave, and how they affect other areas in the compartment, is essential.

Figure 3.1 Laboratory test of a column in a localised fire[15]

3.1 Existing work and implementation in the Eurocode

Performance-based fire engineering using localised fires is covered by Annex C of EN 1991-1-2[2]. This Annex gives a method for calculating the flame length and temperatures in the plume of a localised fire. It is based on work by Heskestad[10] and Hasemi[11], which provides a correlation between fire size (defined by the rate of heat release and diameter) and other parameters, including the flame height and the internal temperature of the fire.

Fires that impact the ceiling tend to spread in a radial direction. The model accounts for this when calculating the temperature distribution within the compartment. Figure 3.2 shows both situations.

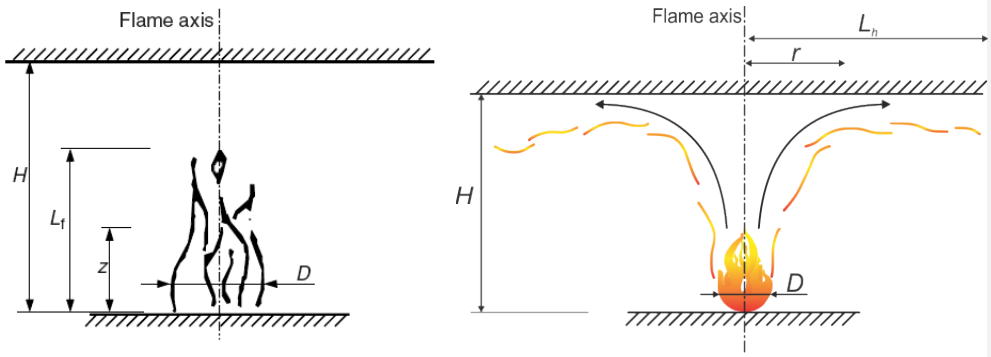

Figure 3.2 Key parameters describing a localised fire (left: fire does not impact the ceiling, right: fire impacts ceiling)

EN 1991-1-2 Annex C does not give a method for assessing the temperature or the heat flux received by a member at a given distance from the fire source. Additionally, the EN 1991-1-2 Annex C method conservatively sets the emissivity of the flame as equal to 1.0, which tends to produce conservative results when compared to tests. Under the European Union's Research Fund for Coal and Steel (RFCS) project LOCAFI, work was carried out to improve the Annex C methodology for localised fires. Through a series of tests, and subsequent numerical and analysis work, refinements to the methodology were proposed, addressing these limitations.

The improved model is introduced in Section 4 and presented in detail in Annex A of this document. Section 3.2 describes the testing that was undertaken to calibrate and verify this model.

3.2 Tests and calibration

This section describes the tests that were undertaken to develop an improved thermal model for localised fires. Full details can be found in the deliverables from the LOCAFI project, as referenced in the text.

3.2.1 Tests at the University of Liège

The first group of tests undertaken as part of the LOCAFI project were performed at the University of Liège. A total of 24 single basin tests were carried out. Full details of the tests can be found in Deliverable 6 of the LOCAFI project[12].

Two kinds of combustible liquids were used, with the tests performed in such a way as to obtain the same heat release rate (HRR). The liquids used were N-Heptane and Diesel.

Tests were performed with and without a column in the centre of the fire pool. The presence of the column did not seem to have a significant effect on the HRR.

Figure 3.3 2 m test pan, showing fuel feed mechanism (from LOCAFI Deliverable 15[13])

The combustible liquid was placed in basins of five different diameters, from 600 mm to 2200 mm. Each diameter was tested with both N-Heptane and Diesel, in identical configurations. Unlike the tests described in 3.2.2, the fuel was delivered to the basin at a fixed rate, rather than starting the test with the full volume of fuel in the basin. This control mechanism allowed the HRR to be kept constant at around 500 kW/m².

The HRR for the Liège tests was computed using Equation (3.1), where 675 is the density of fuel (kg/m^3) and 44000 the enthalpy of combustion (kJ/kg). This formula is presented in LOCAFI deliverable D8[Error! Bookmark not defined.].

$$HRR = \frac{Flow}{60} \times \frac{675}{1000} \times 44000 \qquad (3.1)$$

Table 3.1 shows a summary of the tests conducted.

Table 3.1 Summary of tests conducted by the University of Liège

Test No.	Diameter (m)	Combustible	Measured HRR (kW)
1	0.6	Diesel	185
2	0.6	Heptane	173
3	0.6	Diesel	154
4	0.6	Heptane	149
5	1.0	Diesel	505
6	1.0	Heptane	485
7	1.0	Diesel	474
8	1.0	Heptane	455
9	1.4	Diesel	979
10	1.4	Heptane	950
11	1.4	Diesel	955
12	1.4	Heptane	921
13	1.4	Diesel	979
14	1.4	Heptane	950
15	1.8	Diesel	1620
16	1.8	Heptane	1569
17	1.8	Diesel	1565
18	1.8	Heptane	1515
19	2.2	Diesel	2421
20	2.2	Heptane	2341
21	2.2	Diesel	2365
22	2.2	Heptane	2292
23	Wood		
24	Wood		

3.2.2 Tests at FireSERT (University of Ulster)

A total of 52 tests were conducted at FireSERT (University of Ulster), encompassing a large range of fire sizes and locations. The tests were divided into 2 series; tests with no ceiling (Table 3.2) and tests with a ceiling (Table 3.3).

Full details of the tests can be found in Deliverable 7 of the LOCAFI project[14].

3.2.2.1 Fire tests with no ceiling

31 tests were conducted as part of the first phase of work (Table 3.2). The distance between the column and fire was varied in order to study different fire loads and location scenarios. Fuel loads were varied in terms of fuel type (Diesel, Kerosene and wooden cribs), overall fire size (number and size of basins) and position. Several different steel columns were also used, allowing the effects of variation in the steel shape or size on the temperatures and fluxes to be measured. The HRR for the different fuels was also measured to improve and extend EN 1992-1-2 Annex C.

A discrepancy was observed between the measured values of heat release and the heat release that would be expected for the combination of fire size and combustible tested. A correction was applied to the measurements for the purposes of numerical modelling, as discussed in LOCAFI Deliverable 8-9[Error! Bookmark not

defined.]. Table 3.2 and Table 3.3 present both the original measurements and the corrected values.

Ally Na
Delete

Table 3.2 Summary of tests conducted by FireSERT, with no ceiling

Test Number	Fuel	Diameter and number of basins	HRR (kW)	
			Measured	Corrected
Column O2 - O1	Kerosene	0.7 m	783	503
Column O2 - O2	Kerosene	0.7 m	728	515
Column O2 - O3	Diesel	0.7 m	640	468
Column O2 - O4	Diesel	0.7 m	543	442
Column O2 - O5	Diesel	0.7 m	485	388
Column O2 - O6	Diesel	0.7 m	640	441
Column O2 - O7	Kerosene	0.7 m	658	493
Column O2 - O8	Kerosene	1.6 m	4378	3492
Column O2 - O9	Kerosene	0.7 m × 4	3388	2665
Column O2 - O10	Diesel	1.6 m	3617	2725
Column O2 - O11	Diesel	0.7 m × 4	2601	2015
Column O2 - O12	Kerosene	1.6 m	3713	2648
Column O2 - O13	Diesel & Kerosene	0.7 m × 2	2899	2428
Column O2 - O14	Wood	0.5 m cubed	1944	1433
Column I2 - I1	Kerosene	0.7 m	737	529
Column I2 - I2	Kerosene	0.7 m	663	484
Column I2 - I3	Kerosene	0.7 m	692	559
Column I2 - I4	Kerosene	0.7 m	806	637
Column I2 - I5	Diesel	0.7 m	688	578
Column I2 - I6	Diesel	0.7 m	658	513
Column I2 - I7	Diesel	0.7 m	547	466
Column I2 - I8	Diesel	0.7 m	676	484
Column I2 - I9	Kerosene	1.6 m	4762	3750
Column I2 - I10	Kerosene	1.6 m	3894	3200
Column I2 - I11	Kerosene	0.7 m × 3	2255	1873
Column I2 - I12	Kerosene	0.7 m × 2	1439	1192
Column I3 - I13	Kerosene	0.7 m	736	570
Column I3 - I14	Kerosene	0.7 m	708	525
Column I3 - I15	Kerosene	0.7 m	617	520
Column I3 - I16	Kerosene	0.7 m × 2	1335	1114
Column H2 - H1	Kerosene	0.7 m	641	438
Column H2 - H2	Kerosene	0.7 m	610	514
Column H2 - H3	Kerosene	0.7 m	628	458
Column H2 - H4	Kerosene	0.7 m	630	484
Column H2 - H5	Kerosene	0.7 m × 2	1425	1106
Column H2 - H6	Kerosene	0.7 m × 3	2402	1771
Column H2 - H7	Kerosene	1.6 m	3828	2955

Figure 3.4 shows two of the tests. The photograph on the left shows the pans used to contain the liquid fuel, which constrain the fire diameter.

Figure 3.4 Test set-up for localised fire tests at FireSERT (left: basins for containing liquid fuel, right: wooden cribs)[15]

3.2.2.2 Fire tests with ceiling

21 additional cases were tested as part of the second phase of work. As in the first phase, the size of the fire and its position within the compartment were varied. This test series is summarised in Table 3.3.

Table 3.3 Summary of tests conducted by FireSERT, with a ceiling

Test Number	Fuel	Diameter	HRR (kW)	
			Measured	Corrected
Ceiling - O21	Kerosene	0.7 m	739	563
Ceiling - O22	Kerosene	0.7 m	759	575
Ceiling - O23	Kerosene	0.7 m	814	511
Ceiling - O24	Kerosene	0.7 m	763	607
Ceiling - O25	Kerosene	0.7 m	476	512
Ceiling - O26	Kerosene	1.6 m	3653	2885
Ceiling - O27	Diesel	0.7 m	515	496
Ceiling - O28	Diesel	0.7 m	397	468
Ceiling - O29	Diesel	0.7 m	633	490
Ceiling - O30	Diesel	0.7 m	614	472
Ceiling - O31	Kerosene	0.7 m × 2	1420	1074
Ceiling - O32	Diesel	0.7 m × 2	1185	952
Ceiling - O33	Wood	0.5 m cubed	440	295
Ceiling - O34	Wood	0.5 m cubed	400	273
Ceiling - O35	Wood	0.5 m cubed × 2	702	666
Ceiling - O36	Wood	1 × 1 × 0.5 m	1410	1870
Ceiling - O37	Kerosene	0.7 m × 4	3215	2506
Ceiling - O38	Wood	1 × 1 × 0.5 m	1788	2253
Ceiling - O39	Diesel	1.6 m	-	-
Ceiling - O40	Kerosene	0.7 m	-	-
Ceiling - O41	Wood	1 × 1 × 0.5 m	-	-

Figure 3.5 shows a flame from test ‘Ceiling - O38’ in which the flame impact on the ceiling is clearly visible.

Figure 3.5 Fire impacting the ceiling

3.2.3 Numerical modelling

In support of the tests, a comprehensive numerical study was carried out. The key aim of the numerical work was to extrapolate the test database to situations outside the scope of the testing work, including fires of increased diameter which would be dangerous to test.

The Fire Dynamics Simulator (FDS)[17] software was used for the numerical work, which simulates heat transfer from a fire based on CFD. Figure 3.6 compares a photograph of the actual flame in a test with a predicted flame using the FDS software.

Fire is a dynamic and variable phenomenon, which is very difficult to predict computationally. FDS therefore requires a number of input parameters, many of which depend on the particular circumstances relating to the test. Model parameters include combustion efficiency, soot yield, radiative loss fraction, turbulence model, turbulence parameters and the number of radiation angles. The most significant input parameters are described in the following sections.

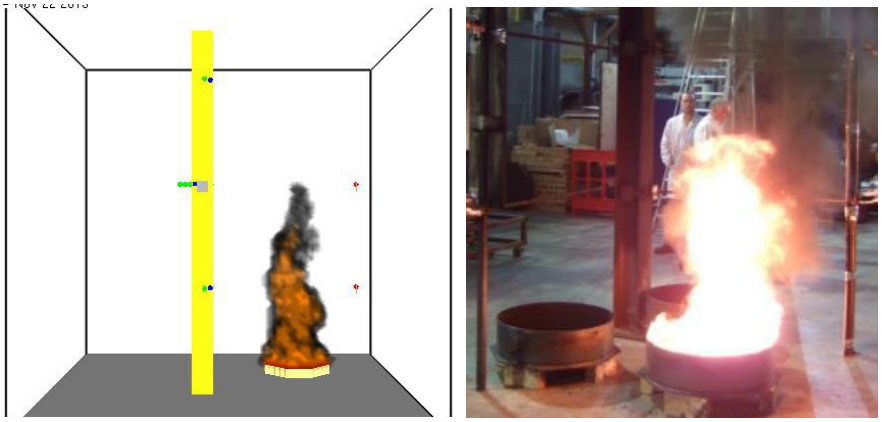

Figure 3.6 Comparison between flame shape prediction by FDS and a photograph of the test, for FireSERT test Column I2 - I11 [17]

3.2.3.1 Turbulence model

The correct reproduction of turbulence (chaotic changes in pressure and fluid velocity) is a fundamentally important part of most CFD problems. In fire, turbulence tends to lead to changes in flame height and position with time. Reproduction of the physical processes involved with turbulence is beyond the capability of any computational model at the current time. Instead, programs like FDS make use of global approximation algorithms, each of which can have different advantages and drawbacks for different situations, depending on the boundary conditions of the problem. FDS 5 uses the relatively old, but well established, 'Smagorinsky' model whereas FDS 6 allows selection of a number of other turbulence models, including the 'dynamic Smagorinsky' model, 'Vreman' model and 'Deardoff' model[15] (which is selected as default).

A number of parametric studies were conducted to explore the variation in the temperatures obtained when each of the different models was employed. Studies also explored the effect of varying the parameters that govern the behaviour within each of the algorithms which make up the model. The eventual conclusion of the study was that the 'Constant Smagorinsky' model produced the best consistency with the test results, with the Smagorinsky constant taken as equal to 0.1.

Designers wishing to employ CFD solutions should be aware that the choice of turbulence model can significantly affect the numerical results.

3.2.3.2 Radiative fraction

The radiative fraction represents the fraction of energy released from the fire as thermal radiation, as opposed to being released through convection. As explained in Section 13.1.1 of the FDS User Guide[Error! Bookmark not defined.], the true proportion of radiative release is a function of the flame temperature and chemical composition, neither of which can be calculated by the program at a high enough resolution for the result to be accurate. Instead, the program uses a global calibrated value.

By default, FDS uses a value of 0.35, i.e. 35% of the heat is radiative and 65% convective. Other values for the radiative fraction were also tested, leading to a different balance between the convective and radiative heat. The best agreement was found with the default value.

3.2.3.3 Cross winds

Numerical simulations are usually based on a perfectly still compartment, meaning air rises vertically upwards, and flames tend to be vertical. In real conditions, this assumption is rarely true, with even the slightest air movement often causing 'tilting' of the flame. Many of the tests described in Sections 3.2.1 and 3.2.2 showed significant tilting; an example is shown in Figure 3.7.

Figure 3.7 Test O36, showing flame tilting[15]

Although not systematically measured during the tests, flame tilting was clearly visible. Thus, the inclusion of wind was fundamental to achieve a high degree of accuracy in model calibration.

3.2.4 Key findings

The LOCAFI tests provide a large body of data on configurations that are currently not covered by EN 1991-1-2 Annex C.

The University of Liège tests focused on configurations where the column is engulfed in the fire. The influence of the presence of a column on the flame height and temperature at different levels was investigated, from which it was demonstrated that the presence of the column produces a higher flame. However, the flame height and temperatures along the vertical axis predicted by EN 1991-1-2 remain on the safe-side with or without a column in the flame (combusting zone) and the plume (non-combusting zone) domains.

The University of Ulster tests focused on configurations where the columns are situated outside the fire. These tests demonstrated that the flame height and temperatures along the vertical axis of the fire source predicted by the EN 1991-1-2 were on the safe side. In addition, these tests provided a large body of data for the calibration of a method for predicting the heat flux received by a column situated

outside the fire. The tests, performed with and without a ceiling, have shown that the wind has a strong influence on the temperatures and heat fluxes measured close to the fire source, while the flux received away from the fire was found to be largely unaffected.

4 NEW MODEL FOR FIRE LOADING ON COLUMNS IN LOCALISED FIRES

4.1 Principles and field of applications

A new model for localised fires has been developed, based on the findings of the test programme described in Section 3. The new model has been verified against heat flux measurements from the test programme, and has been found to give acceptably conservative results in all cases.

The key concept is the discretisation of the fire into a virtual solid flame, constructed from cylinders and rings in its simplest form or smooth shapes in advanced modelling (Figure 4.1).

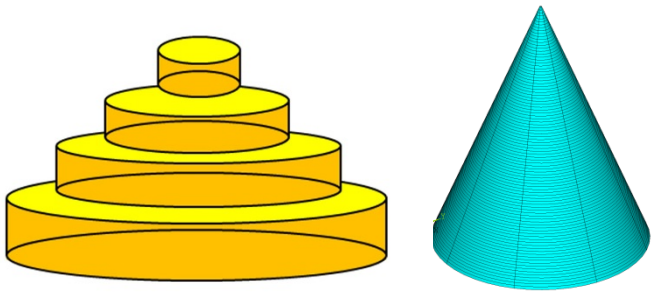

Figure 4.1 Modeling of a localised fire using a cylindrical or a conical discretisation

The radiative flux from the virtual solid flame can be calculated at any point in space using standard radiation heat transfer modelling techniques. Once the flux is known, the temperature of a steel column at any position in the compartment can be determined.

If the column is within the flame, the temperature is governed mainly by convective heat transfer, whereas if the column is outside the flame, the temperature is mainly governed by radiative heat transfer (Figure 4.2).

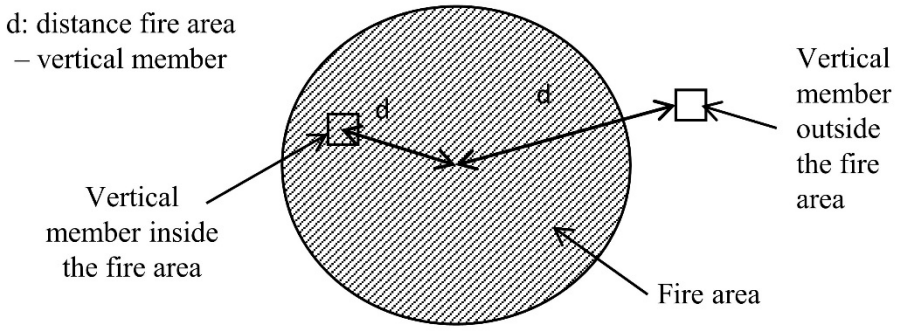

Figure 4.2 Relative position of the fire and the column

The model assumes that the shape of the fire on the ground is circular and is intended for localised fires that do not exceed a diameter of 10 m and a HRR of 50 MW.

The level of heat flux received by a column depends on which of the following four zones it is situated in:

1) Outside the fire,
2) Inside the fire,
3) Inside the fire, in the smoke layer,
4) Outside the fire, in the smoke layer,

An illustration of the four zones is shown in Figure 4.3.

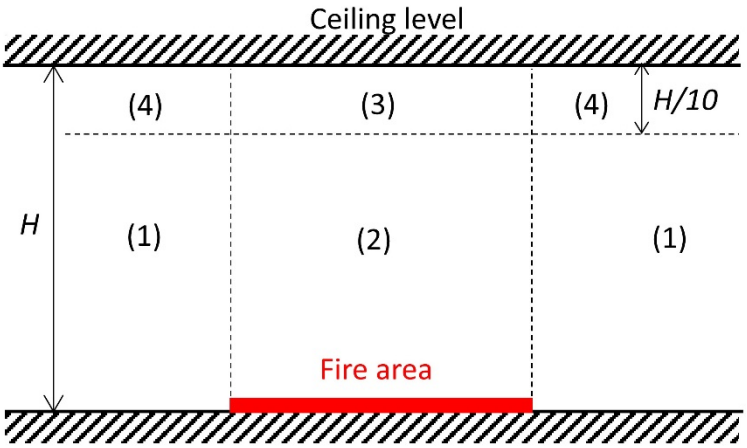

Figure 4.3 Zones for modelling the effects of a localised fire

Before the LOCAFI project, several models were available for zones 2, 3 and 4 but no model was available for zone 1.

The new model covers all situations with a special emphasis on zone 1 and is described in detail in Annex A of this document. Section A.2 describes the model for columns outside the fire area i.e. zones 1 and 4. Section A.3 describes the model for columns within the fire area, zones 2 and 3.

Most fires are conical in shape. However, the centre of the cone may move in response to the wind. For this reason, zones 2 and 3 are approximated as cylinders, with their sides aligned with the edge of the fire.

The recommended value for the height of zones 3 and 4 is $H/10$ but this can be adapted as stated in Annex A.

The method is divided into two global steps; calculation of the incident heat flux received by a segment of the column, then calculation of the temperature of the segment.

4.2 Design tools for modelling localised fire heat fluxes

The analytical model describing the thermal behaviour of steel columns in a localised fire is quite complex and not suitable for use in the design office. This section describes four design tools which implement the model in Annex A of this document.

4.2.1 Contour plots

4.2.1.1 Introduction

This section describes a fast method for computing heat fluxes, based on contour plots. The plots have been generated using the model describes in Annex A, and allow the user to compute the heat flux for the location of interest, without the need to perform detailed calculations.

The contour plots show the heat flux at set distances away from a fire (described by its diameter and HRR) in the vertical and horizontal direction.

Heat fluxes for zone 2 are also presented in the plot, calculated in accordance with the model by Heskestad (as described in Section A.3).

Contour plots for a number of other cases can be found in Annex C.

4.2.1.2 Use of contour plots in design

In order to use a contour plot, a designer must simplify the design fire scenario as follows:

Step a) The shape of the fire is represented as an equivalent circular area,

Step b) The column is modelled as an equivalent rectangular profile (Annex G of EN 1991-1-2[2]),

Step c) The column is rotated so that the widest face of the rectangle is normal to the fire.

Step a)

If the main combustible involved in the localised fire is not circular, then it should be modelled as a circle with a diameter which gives an equal area on the ground, according to Equation (4.1):

$$D_{fire} = \sqrt{\frac{4S}{\pi}} \quad \text{m} \qquad (4.1)$$

Where:

D_{fire} equivalent diameter (m)

S area of localised fire (m²)

For complex shapes, or shapes with an aspect ratio (length/width) above 2, it is recommended that the fire area is subdivided into smaller fires that can be more readily approximated as circular areas. The fluxes from the multiple fires may be added together, as discussed in Section A.4.

Step b)

A rectangular envelope should be drawn around the cross-section of the column, regardless of its original cross-section (Figure 4.4). This approach is consistent with the assumptions made in Annex G of EN 1991-1-2. Simplification of section geometry avoids the need to consider complex phenomena such as the shadow effect (when part of a cross-section "shades" other parts from incident radiation).

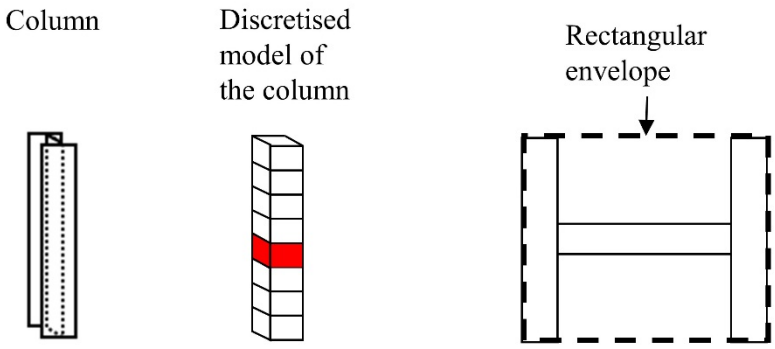

Figure 4.4 H-column modelling and detailed modelling of a segment of a column

Step c)

The orientation is defined with respect to a line that joins the column to the centreline of the fire source (Figure 4.5).

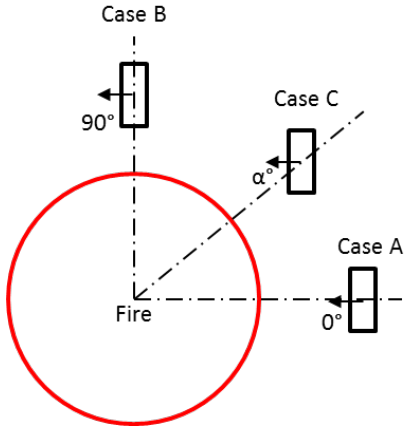

Figure 4.5 Possible orientations of the column

For the purposes of design, the column should be rotated so that the widest face of the rectangular envelope is normal to the centreline, which represents the most conservative assumption (Case A in Figure 4.5). The point of computation for all the faces is conservatively taken at the centre of the face normal to the fire; this is discussed in Section B.1.2.

The distance along the x-axis is taken as the length between the centre of the column face and the centre of the fire.

In the likely event that there is not a contour plot giving the exact properties of the equivalent fire, the contour plot with the next highest HRR and diameter should be selected, which gives a conservative result.

Once the flux values have been read from the contour plot, the mean radiative heat flux received by the section can be calculated using Equation (4.2). The values are weighted in accordance with the widths of the faces.

$$\dot{h}_{m,r} = \frac{l_1 \dot{h}_{r,1} + 2l_2 \dot{h}_{r,2}}{2l_1 + 2l_2} \qquad (4.2)$$

Where:

$\dot{h}_{m,r}$ is the mean radiative heat flux received by the section

$\dot{h}_{r,1}$ is the heat flux received by face 1 of the section, read from the appropriate contour plot

$\dot{h}_{r,2}$ is the heat flux received by face 2 of the section, read from the appropriate contour plot

As a conservative simplification, the heat flux for the 90° faces may be taken as 50% of the heat flux received on the 0° face.

For columns with faces that are not oriented normal to the fire, as shown in Case C of Figure 4.5, the widths of the faces require adjustment before the contour plots can be applied, as shown in Figure 4.6.

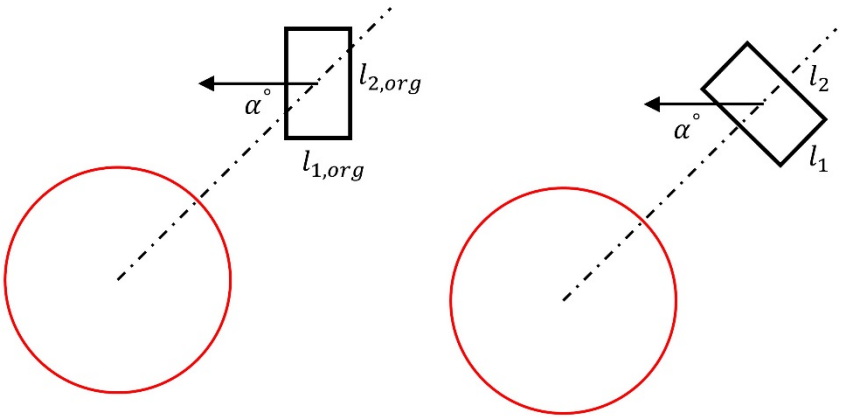

Figure 4.6 Adjustment for columns which are not orientated normal to the fire

The original widths are $l_{1,org}$ and $l_{2,org}$. The adjusted widths are given by

$$l_2 = l_{1,org} \times \sin\alpha + l_{2,org} \times \cos\alpha \qquad (4.3)$$

$$l_1 = (l_{1,org} + l_{2,org}) - l_2 \qquad (4.4)$$

The flux is then calculated in accordance with Equation (4.2).

The contour plots assume that the flame is not impacting the ceiling. If the flame is found to impact the ceiling (by application of Equation (A.2)), the designer should additionally consider the 'hot zone' (zone 4 on Figure 4.3). The heat flux in this zone should be calculated using Equation (A.21). For most designs, the heat flux in zone 4 will be higher than in zone 1 (covered by the contour plots). Hence, the highest temperature in the column, which should be used in the resistance calculations in Section 5, will be in zone 4.

4.2.2 Spreadsheet tools

Greater precision can be obtained by performing the calculation using a spreadsheet, using the model presented in Annex A and B of this document. A spreadsheet can take into account the actual view factors between the fire and the faces of the section. Examples of spreadsheet calculations are shown in Figure B.9 and Figure B.11

As thermal transfer is a complex process, the equations required are numerous and lengthy. It is recommended that the calculation is not implemented by non-experts.

4.2.3 OZone

As an alternative to the designer performing a hand calculation or developing their own analysis tool, a number of software tools have been developed that implement the LOCAFI thermal model. One readily available tool for this purpose is OZone.

OZone is a user-friendly software which calculates the thermal actions generated by a fire and the evolution of temperature in a structural steel member. OZone includes nominal fire curves and two types of natural fire models: localised fires and compartment fires. OZone (along with other software related to fire developed by ArcelorMittal) can be found here:

http://sections.arcelormittal.com/download-center/design-software/fire-calculations.html

For compartment fires, OZone enables the use of one-zone or two-zone fire models, as defined in Annex D of EN 1991-1-2. The main assumption in zone models is that the compartments are divided into zones in which the temperature distribution is uniform at any time. In one-zone models, the temperature is considered as uniform within the whole compartment. This type of model is thus valid for fully developed fires. Two-zone models are more appropriate when the fire remains confined. In this case, the two-zone model better represents the distribution of temperature in the compartment, with a hot layer close to the ceiling and a cold layer below.

In open spaces or large compartments, where flashover does not occur, the behaviour of the structure must be analysed under localised fire conditions. The localised fire procedure implemented in OZone is based on the LOCAFI model.

As discussed in Section A.2.1.1, the major radiative heat exchanges are modelled by representing the fire as a virtual solid flame that radiates in all directions. The first step of this calculation defines the geometry of the virtual solid flame representing the localised fire and the distribution of temperature as a function of time.The shape of the virtual solid flame may be cylindrical or conical. The cylindrical shaped flame is a simpler model, but usually overestimates radiative heat fluxes. OZone implements a conical shape for the virtual solid flame which has been shown to predict the heat flux more accurately.

For cases where the flame is taller than the ceiling level, the cylinder or the cone must be taken as the ceiling height. An additional radiant ring, representing the spreading of the flame under the ceiling should be considered outside the cylinder or cone.

The radiative calculation is implemented in OZone without the use of surface integrals (as used in SAFIR, see Section 4.2.4). Instead, the model is based on configuration factors appropriate for the element shape, as shown in Equation (A.9).

The flux is calculated separately for the 4 faces of the box perimeter of the profile and an average value of this flux is applied to the whole perimeter of the steel section. This means that the shadow effect is not taken into account. The coupling between a localised fire and a compartment fire allows a combination of the influences of the radiative heat fluxes.

The input required for a localised fire includes the position, diameter and evolution of HRR with time for a maximum number of 5 fires.

For natural fire models, several scenarios can be used. For compartment fires, it is necessary to define both the compartment and the fire characteristics, using Annex E of EN1991-1-2 or a user defined fire.

If no compartment is defined, it is assumed that a localised fire develops in open space.If a compartment is defined together with a localised fire, OZone calculates the hot and cold zone temperatures in the compartment considering automatically the maximum fire area as the sum of the areas of the localised fires. For the temperature calculation, OZone proposes three options: hot-zone temperature, localised fire temperature, or the maximum of either (given in the software as 'Maximum Between Both').

4.2.4 Finite element models

If the designer desires a greater level of accuracy, finite element (FE) software such as SAFIR® or ANSYS® may be used. Use of an FE model reduces the number of simplifications that need to made and has the following advantages:

- A more precise conical shape for the virtual solid flame approximation can be assumed, instead of a succession of cylinders and rings.
- The real shape of the column can be considered, including the shadow effect on radiative transfer.
- The view factors between each face and the radiating virtual solid flame can be calculated independently.
- A non-uniform temperature profile may be calculated throughout the cross-section
- Coupled thermal-mechanical behaviour may be considered. An example of this is the thermal bowing of a column heated asymmetrically.

Different software packages may implement the model in different ways, particularly in the level of discretisation. To explore the issues that must be considered for implementation, a short description of the approach implemented in SAFIR is provided here.

Two flame shapes are implemented in SAFIR; cylindrical and conical. The user is free to choose either, depending on their preference. An example of the conical flame is shown in Figure 4.7.

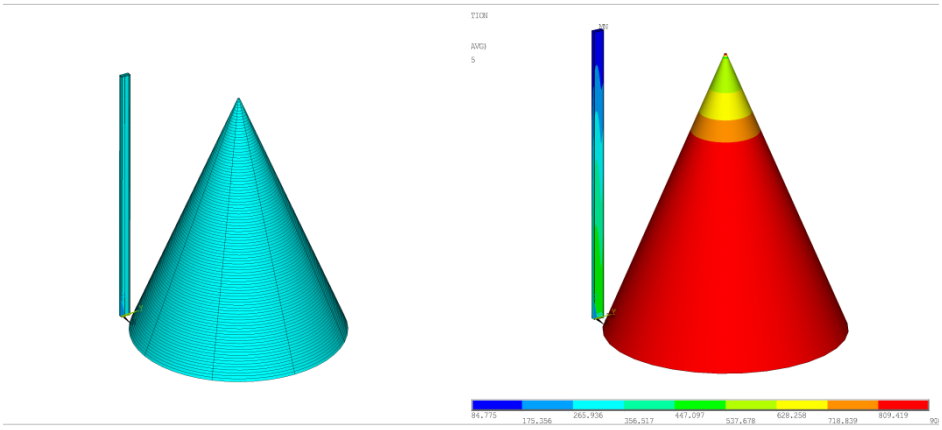

Figure 4.7 Flame shape (left) and surface temperature (right) in SAFIR

The thermal model of SAFIR calculates the temperature by a series of 2D thermal analyses performed at each longitudinal point of integration of each structural finite element chosen by the user. These elements can have any orientation in space.

The heat flux at any time is calculated separately for each face of the finite element. This means that the impinging flux from the local fire to the finite element is anisotropic; the faces that are orientated towards the fire receive the highest flux, while the faces on the opposite side receive no flux at all.

When a flux from a localised fire is calculated on a face, heat losses are automatically added from the face to the far field, which is assumed to be at ambient temperature.

The fire source is divided into horizontal slices of equal depth of 0.1 m. This is smaller than the value of 0.5 m recommended for hand calculation (see Section A.2.1.1). Each slice and each ring is divided into 36 sectors of 10 degrees each. These divisions define a series of facets that form the outer face of the flame. The radiative flux from each facet is calculated to each face of the section.

The structure can be subjected to one or several local fire sources. In case of multiple fires, the fluxes from each fire are added together.

4.3 Determination of the temperature of a segment of the steel column

This section describes the process of calculating the temperature of a segment of a column, based on the impinging flux. As described in Section 5, member design requires temperatures rather than fluxes.

The heat release rate (HRR) can be determined from EN 1991-1-2 Annex E, which divides the HRR curve (see Figure 4.8) into 3 parts: a growing phase, a constant phase (if any) where the fire is fuel or ventilation controlled, and a decaying phase. With this shape of curve, the most critical phase in terms of thermal actions is the constant phase.

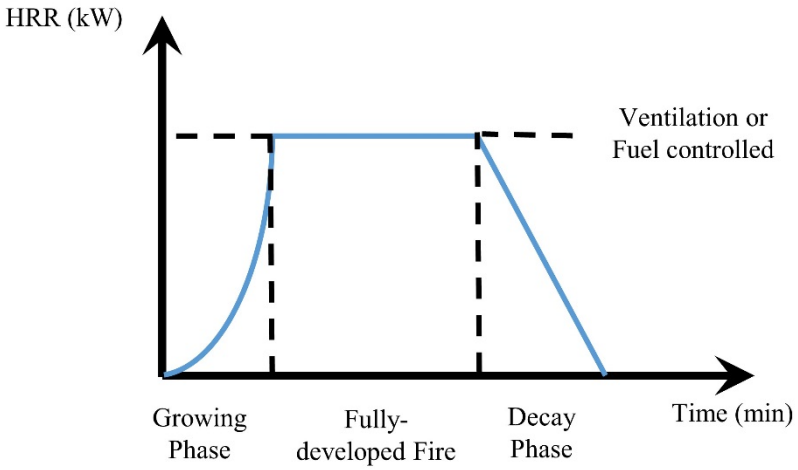

Figure 4.8 HRR curve calculated according to Annex E of EN 1991-1-2

Heat release from a fire is a time dependent relationship, which suggests that flux should be computed at a number of time steps. Taking also into account the fact that the heat flux varies up the length of the column, the number of calculations increases considerably.

As a segment begins to receive flux from the fire, its temperature will rise. In the fuel-controlled phase, the flux remains constant, meaning a point will eventually be reached where the flux received by the segment is balanced by the flux radiated to the surrounding environment. This is known as the steady-state temperature.

If the segment has a large volume, the time taken to reach the steady-state temperature may be long. In many cases the time required to reach the steady-state is longer than the duration of the fire, meaning the steady-state is never reached.

The designer may conservatively assume that the steady-state is always reached. This significantly reduces the computational effort required, since the time dependency of the calculation is removed. However, the steady-state temperature that is assumed to be reached may be considerably higher than the temperature that is actually reached. Designers who are prepared to perform a more advanced analysis, taking into account the dependency on time, are likely to achieve a more cost-efficient design. The advanced method is referred to below as the 'incremental method', in Section 4.3.2.

The recommended method for assessment of the temperature depends on the precision with which the flux is calculated. For each of the four methods presented in Section 4.2 the following is recommended:

- For contour plot calculations, the total heat flux is given for the constant phase. The temperature is calculated according to the equations presented in Section 4.3.1.
- For spreadsheet calculation, it is recommended to compute the total heat flux received by a segment of the column for the following values of the HRR: 25%, 50%, 75% and 100% of the maximum. The temperature should then be calculated using the incremental method (Section 4.3.2).
- Ozone performs the calculation is accordance with the incremental method. No additional input parameters are required.

- FE software will be capable of calculating both heat fluxes and temperatures in the same analysis.

As different segments located at different levels up the height of the column receive different fluxes, this will result in different temperature distributions from level to level. These differences will lead to a longitudinal conductive heat flux up the column that will tend to equalise the steel temperature in adjacent segments. Taking this effect into account would require a 3D model of the column. Several numerical analyses have demonstrated that this effect is quite limited, and the actual temperature distribution is sufficiently well approximated by a series of 2D thermal analyses performed at different levels, each with the boundary conditions that prevail at that level.

4.3.1 Steady-state method

Knowing the mean radiative heat flux received by a segment, its steady state temperature can easily be computed from equations in the Eurocodes.

As the segment is outside the fire, the convective exchange will be with ambient air (20°C), except if coupled with a compartment fire. For radiative exchange, the section will absorb $\varepsilon\dot{h}_{m,r}$ and will radiate toward the environment.

The heat balance equation is therefore:

$$0 = \alpha_c(\theta - 20) + \sigma\varepsilon[(\theta + 273)^4 - (20 + 273)^4] - \varepsilon\dot{h}_{m,r} \qquad (4.5)$$

Where:

α_c is the coefficient of heat transfer by convection = 35 W/(m²K) in accordance with EN 1991-1-2

σ is Stefan-Boltzmann's constant, equal to 5.67×10^{-8} W/(m²K⁴)

ε is the emissivity of the steel (EN 1993-1-2 gives a value of 0.7)

θ is the steel temperature, in °C

The steady-state temperature is independent of the size of the segment on which the flux is impinging.

This equation may be solved iteratively, leading to a relationship between θ and $\dot{h}_{m,r}$. Assuming the recommended values of σ and ε, Equation (4.5) may therefore be plotted, as shown in Figure 4.9.

Ally Na
Forma
spellin
Ally Na
Delete
Ally Na
Delete
Ally Na
Forma
spellin

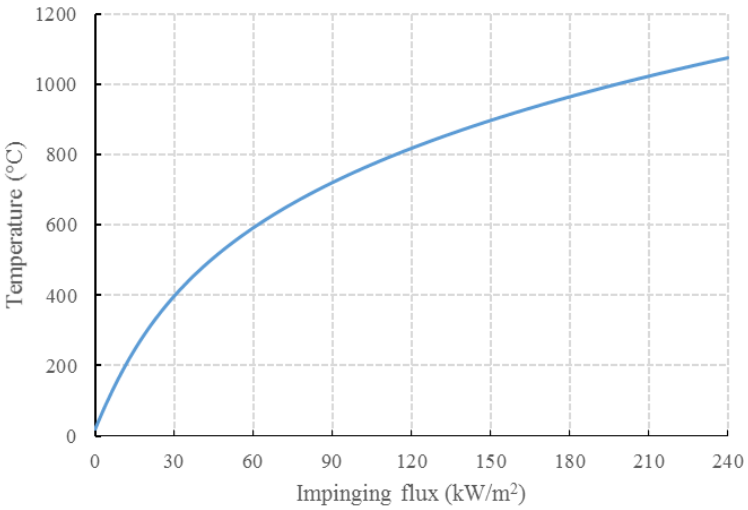

Figure 4.9 Relationship between steady-state temperature and impinging heat flux

4.3.2 Incremental method

Once the incident heat flux has been calculated, the incremental method described in EN 1993-1-2 can be used to determine the time-temperature relationship. The temperature of a section depends on the net heat flux, which is the difference between the incident heat flux and the emitted heat flux. The net heat flux is given by the thermal balance equation, of which Equation (4.6) is a special case:

$$\rho C_p(T)\frac{dT}{dt} = \frac{A_m}{V}\left[\dot{h}_{z_j} - \alpha_c(T-20) - \sigma\varepsilon((\theta+273)^4 - 293^4)\right] \qquad (4.6)$$

Where:

$\dot{h}_{z_j}$ is the net heat flux received by the section (described in Annex A)

ρ is the density of steel, in kg/m^3

C_p is the specific heat of steel, in J/(kgK)

A_m/V is the section factor of the segment, in m^{-1}

From this equation, the temperature is computed in an incremental way using a time step Δt (for example 60 s) with:

$$T^{t+\Delta t} = T^t + \Delta t\frac{A_m}{V}\frac{1}{\rho C_p(T^t)}\left[\dot{h}_{z_j} - \alpha_c(T-20) - \sigma\varepsilon((\theta+273)^4 - 293^4)\right] \qquad (4.7)$$

Where:

$T^{t+\Delta t}$ is the temperature of segment z_j at time $t+\Delta t$.

All time dependent quantities on the right-hand side must be evaluated at time t as the HRR varies with time. This equation may be easily implemented in an excel spreadsheet. OZone's temperature computations are based on this method.

5 COLUMN DESIGN

EN 1993-1-2 and EN 1994-1-2 give models to assess the mechanical resistance of a structural member and integrity criteria that need to be satisfied when exposed to a nominal or natural fire curve. They define the design values of mechanical and thermal material properties in relation to characteristic values. The design values are given by the characteristic values divided by the partial factor $\gamma_{M,fi}$. However, since the recommended value of $\gamma_{M,fi}$ = 1.0 is accepted by all the National Annexes, thermal properties are usually referred to without any designation as characteristic or design values.

5.1 Verification

The verification is expressed as the requirement, at time *t* during the fire exposure, that:

$$E_{\mathrm{fi,d,t}} \leq R_{\mathrm{fi,d,t}} \tag{5.1}$$

The effects of indirect actions (internal forces and moments induced in the structure by deformations and restrained thermal expansion) do not need to be considered when fire safety is based on the standard temperature-time curve. In other cases, indirect actions need not be considered when the effect is identified as being negligible or when the boundary conditions or design model are conservative.

5.2 Load

As a simplification, the value of $E_{\mathrm{fi,d}}$ for member analysis may be taken as:

$$E_{\mathrm{fi,d}} = \eta_{\mathrm{fi}} E_{\mathrm{d}} \tag{5.2}$$

Where:

E_{d} is the design value of the effect of the fundamental combination of actions (ultimate limit state) as given in EN 1990

η_{fi} is a reduction factor for the design load level

The value of the reduction factor η_{fi} will depend on whether Equation 6.10 or 6.10a and 6.10b, given in EN 1990, is used for the fundamental combination.

If Equation 6.10 of EN 1990 is used for the fundamental combination the reduction factor η_{fi} is given by:

$$\eta_{fi} = \frac{G_k + \Psi_{1,1} Q_{k,1}}{\gamma_G G_k + \gamma_{Q,1} Q_{k,1}} \tag{5.3}$$

If Equations 6.10a and 6.10b are used for the fundamental combination the reduction factor η_{fi} is given by the smaller value of the following two expressions:

$$\eta_{fi} = \frac{G_k + \Psi_{1,1} Q_{k,1}}{\gamma_G G_k + \gamma_{Q,1} \Psi_{0,1} Q_{k,1}} \tag{5.4}$$

$$\eta_{fi} = \frac{G_k + \Psi_{1,1} Q_{k,1}}{\xi \gamma_G G_k + \gamma_{Q,1} Q_{k,1}} \quad (5.5)$$

Where:

G_k is the characteristic value of the permanent action

$Q_{k,1}$ is the characteristic value of the leading variable action

ξ is a reduction factor for unfavourable permanent actions, as given in EN 1990

$\Psi_{0,1}$ is a combination factor for the value of a variable action

$\Psi_{1,1}$ is a frequency factor for the value of a variable action

It should be noted that the reduction, frequency and combination factors are Nationally Determined Parameters, and therefore vary from country to country. Designers should ensure that they are using the correct values.

5.3 Resistance

For a member with a non-uniform temperature distribution, the resistance may be taken as that for a uniform temperature equal to the maximum temperature in the member at the time considered.

The temperature θ of the member is determined in accordance with the methods described in Section 4. The temperature of a column should be determined at a number of heights, with the highest temperature used to determine the resistance of the column.

Modelling has shown that the maximum temperature tends to occur at around 1/3 of the column height, assuming the flame is not impacting the ceiling. When the flame is impacting the ceiling, the maximum temperature is likely to be in the hot zone (zone 4 of Figure 4.3).

Ally Na
Delete

5.3.1 Section classification

As for normal temperature design, all cross sections that act wholly or partly in compression are classified in order to establish the appropriate design resistance of the cross section.

As the strength and the elastic modulus of steel reduce at different rates in fire conditions, the section classifications at elevated temperature may differ from those for normal temperature design.

However, rather than determine classification at each elevated temperature, a single classification is made, based on normal temperature behaviour. The classification is carried out using the rules in EN 1993-1-1 except that the value of ε for fire conditions is given by EN 1993-1-2 clause 4.2.2 as:

$$\varepsilon = 0.85 \sqrt{\frac{235}{f_y}} \quad (5.6)$$

where f_y is the yield strength at 20°C.

The coefficient 0.85 takes account of the variation of material properties at elevated temperatures and is an approximation for $\sqrt{k_{E,\theta}/k_{y,\theta}}$. It is possible for a

column to be a more onerous class in fire than at room temperature e.g. Class 3 at room temperature and Class 4 in fire.

Rules for calculating the resistance of Class 4 cross-sections in fire are presented in EN 1993-1-2[3]. Further discussion on this topic is outside the scope of this guide.

5.3.2 Flexural buckling resistance

The design buckling resistance of columns of Class 1, 2 or 3 with a uniform temperature θ_a at time t is determined in a similar manner as for normal temperature design but with adjustments for reduced properties at elevated temperatures. The design resistance is given by EN 1993-1-2 clause 4.2.3.2 as:

$$N_{\mathrm{b,fi,t,Rd}} = \chi_{\mathrm{fi}} A k_{\mathrm{y},\theta} \frac{f_{\mathrm{y}}}{\gamma_{\mathrm{M,fi}}} \tag{5.7}$$

The reduction factor for flexural buckling χ_{fi} is the lower of the values about the y-y and z-z axes, determined as follows:

$$\chi_{\mathrm{fi}} = \frac{1}{\varphi_\theta + \sqrt{\varphi_\theta{}^2 - \overline{\lambda}_\theta{}^2}} \tag{5.8}$$

Where:

$$\varphi_\theta = \frac{1}{2}\left(1 + \alpha\overline{\lambda}_\theta + \overline{\lambda}_\theta{}^2\right) \tag{5.9}$$

With:

$$\alpha = 0.65\sqrt{\frac{235}{f_{\mathrm{y}}}} \tag{5.10}$$

The non-dimensional slenderness at a uniform temperature θ_a is given by:

$$\overline{\lambda}_\theta = \overline{\lambda}\sqrt{\frac{k_{\mathrm{y},\theta}}{k_{\mathrm{E},\theta}}} \tag{5.11}$$

Where:

A	is the cross-sectional area of the steel column
$k_{\mathrm{y},\theta}$	is the temperature dependent reduction factor for steel strength
$k_{\mathrm{E},\theta}$	is the temperature dependent reduction factor for the steel elastic modulus
f_{y}	is the yield strength of the steel
$\overline{\lambda}$	is the non-dimensional slenderness at normal temperature

The reduction factors $k_{\mathrm{y},\theta}$ and $k_{\mathrm{E},\theta}$ are temperature dependent. Numerical values are presented is EN 1993-1-2[3] and are shown in Figure 5.1.

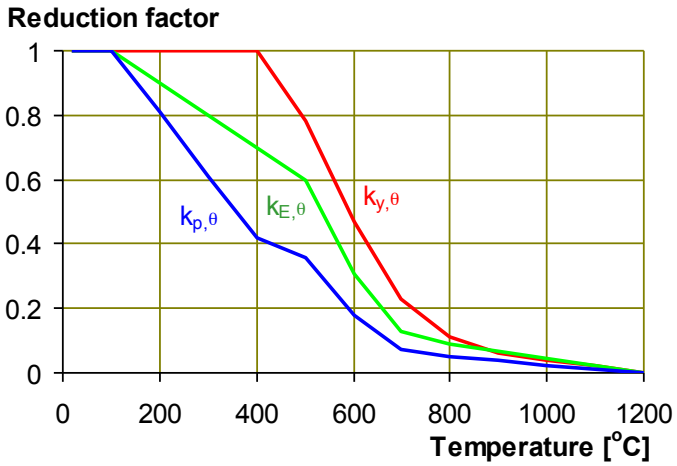

Figure 5.1 Reduction factors for stress-strain relationship of carbon steel at elevated temperatures

5.3.3 Buckling lengths

EN 1993-1-2 clause 2.3.2(3) recommends that the non-dimensional slenderness $\overline{\lambda}$ is determined as for normal temperature design except that, for braced frames, the buckling length l_{fi} may take account of end restraint, as shown in Figure 5.2, provided that each storey of the building comprises a separate fire compartment, and that the fire resistance of the compartment boundaries is not less than that of the column. Because the continuing columns are much stiffer than the column in the fire compartment, it is assumed that they cause the end(s) of the heated column to be restrained in direction.

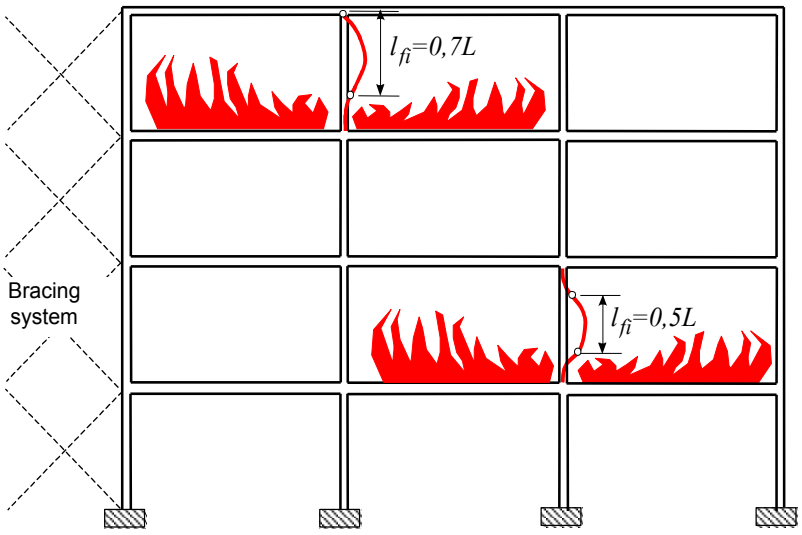

Figure 5.2 Buckling lengths of columns in fire.

5.4 Resistance calculation by FE analysis

As an alternative to the mechanical model described in Section 5.3, the resistance of a column may also be determined using FE analysis.

The FE software selected by the designer must be capable of performing a 'coupled' analysis, where the thermal and mechanical components of the analysis are calculated simultaneously.

The thermal analysis must be performed using a solver capable of calculating the heat flux received from an emitting 'solid flame'. The shape of the flame is defined according to the equations presented in Section A.2. CFD capabilities are not required. This is discussed further in Section A.2.1.1.

For the mechanical part of the analysis, a non-linear material model is recommended. Depending on the preference of the user, beam elements or shell elements may be used. In both cases, care should be taken to ensure that the effects of initial imperfections are accounted for. Further guidance on FE modelling can be found in EN 1993-1-5 Annex C[16].

6 REFERENCES

1 EN 1990 (2002): Eurocode 0: Basis of structural design

2 EN 1991-1-2 (2002): Eurocode 1: Actions on structures - Part 1-2: General actions - Actions on structures exposed to fire

3 EN 1993-1-2 (2005): Eurocode 3: Design of steel structures - Part 1-2: General rules - Structural fire design

4 EN 1994-1-2 (2005): Eurocode 4: Design of composite steel and concrete structures - Part 1-2: General rules - Structural fire design

5 Wang, Y., Burgess, I., Wald, F. and Gillie, M. (2012) Performance-Based Fire Engineering of Structures, CRC Press. Taylor & Francis Group

6 Lennon, T. (2011) Structural Fire Engineering, , ICE Publishing

7 Franssen, J. M. and Vila Real, P. (2015) Fire design of steel structures, 2nd Edition, ECCS Eurocode Design Manuals, Wiley VCH

8 Simms, W.I. (2012) Fire resistance design of steel framed buildings. P375, The Steel Construction Institute

9 Guide to the advanced fire safety engineering of structures (2007), Institution of Structural Engineers.

10 Heskestad, G. (1972) Similarity relations for the initial convective flow generated by fire, ASME Paper 72-WA/HT-17.

11 Hasemi, Y. and Tokunaga, T. (1984) Flame geometry effects on the buoyant plumes from turbulent diffusion flames, Fire Science & Technology 4(1):15-26

12 Franssen, J.M. and Scifo, A. (2013) LOCAFI D6: Description of all parameters that characterise the tests - ULg. (Part of 'Temperature assessment of a vertical steel member subjected to Localised Fire' RFCS project)

13 Nadjai, A. and Sanghoon, H. (2016) H, LOCAFI D15: Background document of the methodology – Ulster. (Part of LOCAFI RFCS project)

14 Nadjai, A. and Sanghoon, H. (2013) LOCAFI D7: Report of all detailed experimental data gathered during localised fire tests - Ulster (Part of LOCAFI RFCS project)

15 Nadjai, A et al., (2018) Experimental and Analysis of Localised Pool Fire Tests on Steel Columns with Compartment Open Ceiling, SiF18 – The 10th

18 Fire Dynamics Simulator (FDS) (2013), FDS Technical Reference Guide, Volume 1: Mathematical Model, https://pages.nist.gov/fds-smv/

19 EN 1993-1-5(2006): Eurocode 3: Design of steel structures – Part 1-5: Plated structural elements

20 Vassart, Olivier et al., (2014) Eurocodes: Background and applications. Structural fire design. Worked examples. EUR Scientific and Technical Research Reports. Publications Office of the European Union. (Available from: https://ec.europa.eu/jrc/en/publication/eur-scientific-and-technical-research-reports/eurocodes-background-and-applications-structural-fire-design-worked-examples)

ANNEX A MODEL FOR CALCULATING FIRE LOADING ON COLUMNS SUBJECT TO LOCALISED FIRES

Considerable test evidence, as described in Section 3.2, has led to the calibration and verification of an analytical model for determining the incident heat flux and temperature rise of a column in a localised fire. The model is described in this Annex.

The physics of heat transfer by both radiation and convection mean that the model is rather complex, and it is not envisaged that designers would attempt to apply the model using hand calculation methods, though implementation in a spreadsheet is possible. Instead, various simplified approaches that implement the principles of the model have been developed, as discussed in Section 4.

A.1 Overview

The temperature of a column subjected to a localised fire can be assessed using the method described below. The method determines the temperature of a segment of a column at a specific height and may be applied multiple times, at any height, in order to construct a temperature profile.

The method is divided into two global steps; calculation of the incident heat flux received by the segment, then calculation of the segment temperature.

It assumes that the shape of the fire on the ground is circular and is intended for localised fires that do not exceed a diameter of 10 m and a HRR of 50 MW.

If the main combustible involved in the localised fire is not circular, then it is modelled as a circle with a diameter which gives an equal area, according to Equation (A.1):

$$D_{fire} = \sqrt{\frac{4S}{\pi}} \quad \text{m} \tag{A.1}$$

Where:

D_{fire} equivalent diameter (m)

S area of localised fire (m²)

The domains of application are shown in Figure 4.3. Section A.2 describes the model for columns outside the fire area (zones 1 and 4) and Section A.3 describes the model for columns within the fire area (zones 2 and 3).

A.2 Column outside the fire area

The flames produced by a localised fire affect an exposed column mainly through radiative heat flux if the column is not engulfed. The flame shape and the relative position of the flame compared to the column have a strong influence over the radiative heat flux received by the column.

For the majority of the volume of the compartment, convective heat flux beyond the fire area can be assumed to be negligible. However, this assumption does not remain true in the smoke layer that spreads under the ceiling. For a localised fire, the height of the smoke layer is generally small compared to the height of the compartment.

If there are some obstructions that can impede the spread of smoke under the ceiling, then the height of the smoke layer $h_{smoke\ layer}$ may be defined by the geometric characteristic of the obstructions (typically the depth of beams). In practice, a value of 10 % of the ceiling height is recommended.

Different expressions for predicting the incident heat flux apply if the location of interest is outside or inside the smoke layer (see Section A.2.1 and A.2.2).

A.2.1 Column outside the smoke layer

The procedure is divided into 3 steps:

(a) Model the geometry of the flame surface,

(b) Calculate the temperature of the flame,

(c) Estimate the radiative incident heat flux on a segment of the steel column.

The convective heat flux is neglected and the radiative heat flux is modelled using the concept of a solid flame, i.e. the flame is seen as a solid surface that radiates heat toward the column.

A.2.1.1 Geometry of the solid flame surface

The first step is to construct the flame surface. A conical shape is assumed, formed by a series of cylinders (vertical faces) and rings (horizontal faces) of decreasing diameter (Figure A.1).

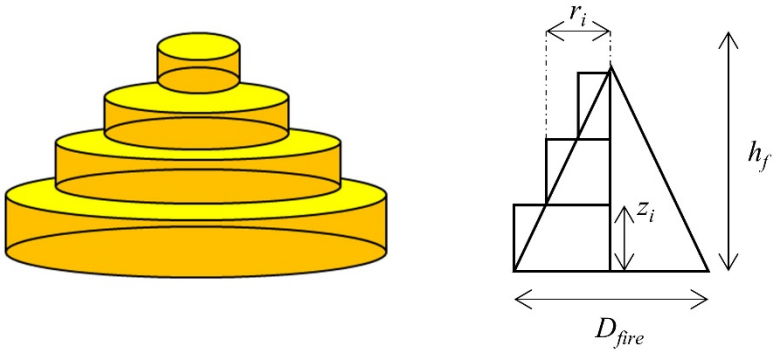

Figure A.1 Solid flame model (left) and geometrical details (right)

The flame height h_f is calculated using the correlation in Annex C of EN 1991-1-2[2]:

$$h_f = -1.02D_{fire} + 0.0148Q(t)^{0.4} \quad \text{(A.2)}$$

Where:

D_{fire} is the diameter of the fire source (m)

$Q(t)$ is the HRR of the fire source (W)

The radius r_i of a cylinder at the height z_i is equal to:

$$r_i = 0.5 D_{fire} \left(1 - \frac{z_i}{h_f}\right) \quad \text{(A.3)}$$

For ease of use, the number of cylinders to model the fire should be limited. A cylinder depth of 0.5 m gives a good balance between precision and usability, and is therefore recommended. A very safe-sided simplification can be made using a cylinder depth equal to the flame height h_f. In that case the solid flame reduces to two components: a cylinder with a disk at the top (diameter = D_{fire}).

A.2.1.2 Radiative properties and temperature of the flame

The second step is the calculation of the radiative properties of the flame and thus the temperature of the solid flame. The temperature of a specific cylinder and ring at a distance z_i along the flame axis (Figure A.2) is assumed constant and equal to:

$$\theta_f(z_i) = \min\left(900;\quad 20 + 0.25\left(0.8Q(t)\right)^{2/3}(z_i - z_{\text{virt}})^{-5/3}\right) \quad \text{(A.4)}$$

Where z_{virt} is the virtual origin, given by:

$$z_{\text{virt}} = -1.02 D_{fire} + 0.00524 Q(t)^{0.4} \quad \text{(A.5)}$$

These formulae are Equations C.2 and C.3 in EN 1991-1-2. The length h_f is defined as the point where the temperature of gases along the flame axis reaches 520°C, according to Equation (A.4).

It is important to note that the HRR varies with time, meaning the characteristics of the flame and the heat fluxes vary during the fire.

It is possible to take into account cases where the fire source is not on the ground but at a different height z_{fire} by adjusting the height under the ceiling (h_{ceil} is replaced by $h_{ceil} - z_{fire}$).

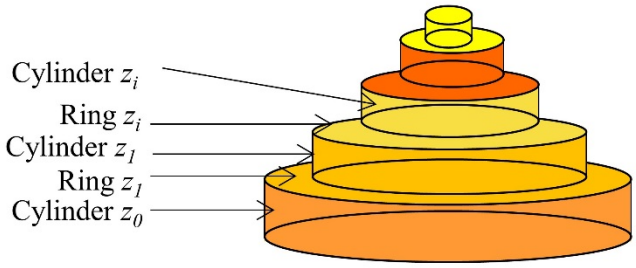

Figure A.2 Simplified model of a fire using rings and cylinders

A.2.1.3 Radiative heat flux received by a segment of the column

Firstly, the cross-section of the column is modelled as a rectangular cross-section, independently of its original cross-section (Figure A.3). This approach is consistent with the assumptions made in Annex G of EN 1991-1-2. Elimination of complex section geometry avoids the need to take into account complex phenomena such as the shadow effect (when part of a cross-section "shades" other parts from incident radiation).

The column is divided into segments (of height z_j) and the heat flux is calculated for each of the four faces of the segment, and then a mean value is calculated.

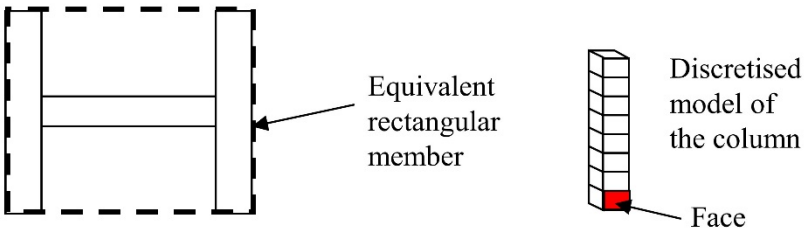

Figure A.3 H-column modelling and detailed modelling of a segment

As it is assumed that the emissivity and the temperature are constant over the surface of each segment, the radiative heat flux can be calculated using a configuration factor, which measures the fraction of the total radiative heat leaving a given radiating surface that arrives at a given receiving surface. Its value depends on the size of the radiating surface, on the distance from the radiating surface to the receiving surface and on their relative orientation. Analytical formulae for configuration factors exist for various scenarios, including the shapes used here for the solid flame.

The configuration factor $\emptyset$ between an infinitesimal plane and a finite cylinder is given by Equation (A.6). The geometrical parameters are shown in Figure A.4.

$$\emptyset_{dA_1 \to A_2} = \frac{S}{B} - \frac{S}{2B\pi}\{L_1 + L_2 + L_3 + L_4 + L_5\} \qquad \text{(A.6)}$$

Where

$$L_1 = cos^{-1}\left(\frac{Y^2 - B + 1}{A - 1}\right)$$

$$L_2 = cos^{-1}\left(\frac{C - B + 1}{C + B - 1}\right)$$

$$L_3 = -Y\left[\frac{A + 1}{\sqrt{(A-1)^2 + 4Y^2}} cos^{-1}\left(\frac{Y^2 - B + 1}{\sqrt{B}(A - 1)}\right)\right]$$

$$L_4 = -\sqrt{C}\frac{C + B + 1}{\sqrt{(C + B - 1)^2 + 4C}} cos^{-1}\left(\frac{C - B + 1}{\sqrt{B}(C + B - 1)}\right)$$

$$L_5 = Hcos^{-1}\left(\frac{1}{\sqrt{B}}\right)$$

Where:

$$S = \frac{s}{r} \qquad X = \frac{x}{r} \qquad Y = \frac{y}{r} \qquad H = \frac{h}{r}$$

$$A = X^2 + Y^2 + S^2$$

$$B = S^2 + X^2$$

$$C = (H - Y)^2$$

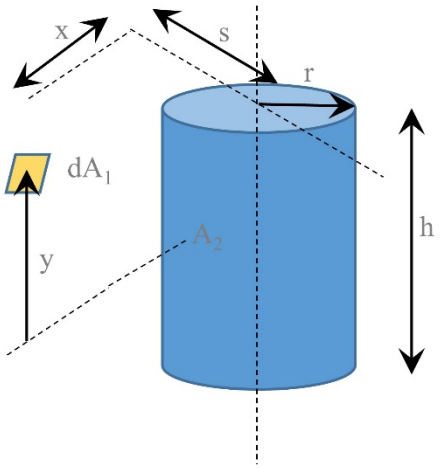

Figure A.4 Geometrical terms used to calculate the configuration factor between an infinitesimal plane and a finite cylinder

The radiative heat flux received and absorbed by $face_j$ from the cylinder z_i is then:

$$\dot{h}_{Cylinder\ z_i \to face_j} = \sigma\varepsilon\left(\theta_f(z_i) + 273\right)^4 . \emptyset_{Cylinder\ z_i \to face_j} \qquad \text{(A.7)}$$

Where:

ε	is the emissivity of the steel (EN 1993-1-2 gives a value of 0.7)
σ	$= 5.67 \times 10^{-8}$ W/(m^{2}K^4)
$\theta_f(z_i)$	is the temperature of cylinder z_i, from Equation (A.4)
$\emptyset_{Cylinder\ z_i \to face_j}$	is the configuration factor of cylinder z_i and the $face_j$ from Equation (A.6)

A model of the fire is shown in Figure A.5.

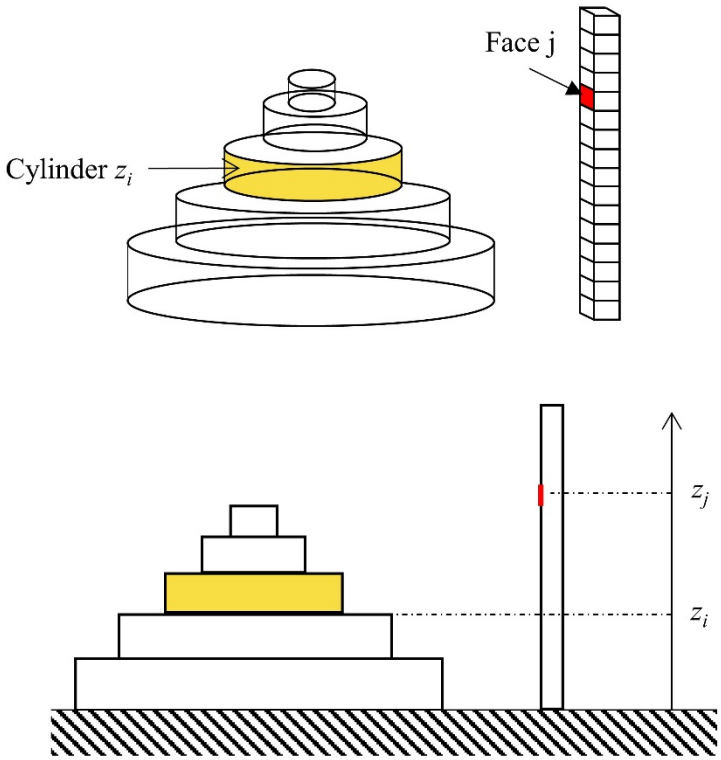

Figure A.5 Radiative exchange between the cylinder z_i and $face_j$ 3d view (above), side view (below)

Configuration factors are additive[2]. For example, the configuration factor $\emptyset$ for the case shown in Figure A.6 can be computed from configuration factors $\emptyset_1$ and $\emptyset_2$:

$$\emptyset_1 = \emptyset + \emptyset_2 \Rightarrow \emptyset = \emptyset_1 - \emptyset_2 \qquad \text{(A.8)}$$

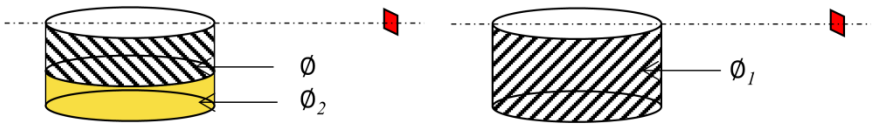

Figure A.6 Additivity rule for configuration factors

Additional rules need to be applied in order to determine the configuration factor and hence heat flux for all possible configurations. Indeed, in the case shown in Figure A.7, face 1 sees the cylinder, faces 2 and 4 partially see the cylinder while no radiative heat flux from the solid flame reaches face 3. Thus, face 1 corresponds to the situation described by Equation (A.6). For face 3, the incident radiative heat flux is zero. The case for faces 2 and 4 is more complex and Equation (A.6) cannot be applied directly because the plane (of the face) cuts the cylinder.

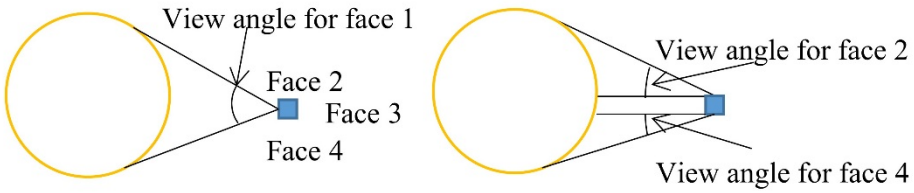

Figure A.7 Example of interaction cylinder – column (top view)

As it is mainly the angle at which the target views the radiative source that controls the radiative heat flux, the adopted solution is to use a surface shape which will lead to an equivalent configuration factor. A cylinder may still be used, but with the modified geometry shown in Figure A.8 and Figure A.9. The diameter of the cylinder is reduced so that the modified cylinder is fully visible by the target face and consequently Equation (A.6) can be used. A more complex case with several cylinders is shown in Figure A.10 which can be handled in a similar way.

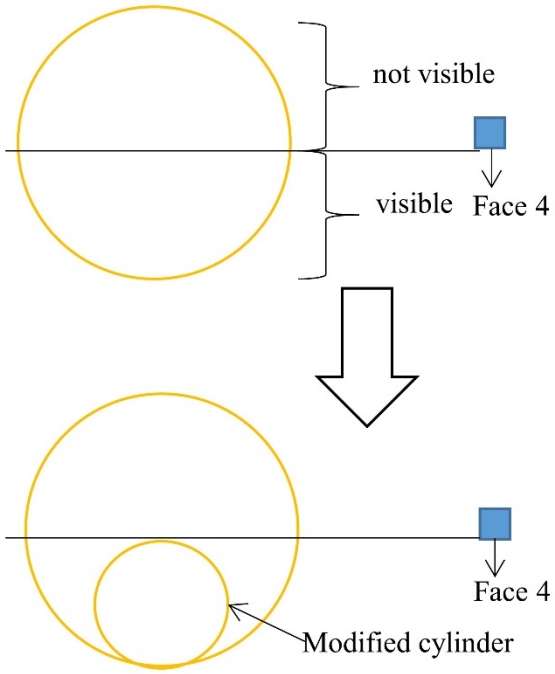

Figure A.8 Cylinder modelling – top view

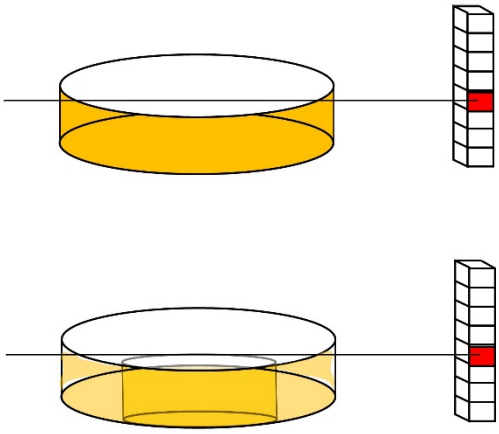

Figure A.9 Cylinder modelling – 3d view

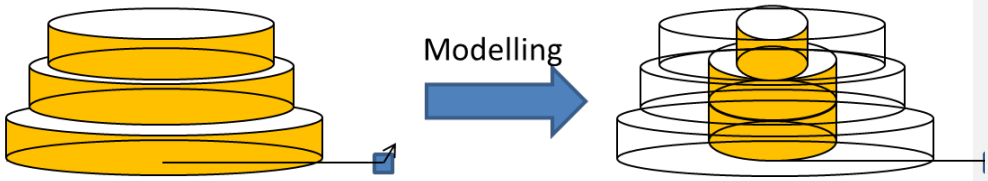

Figure A.10 Complex case of cylinder modelling

The configuration factor between an infinitesimal plane element and a ring in a perpendicular plane is given by Equation (A.9). The geometrical parameters are shown in Figure A.11.

$$\emptyset_{dA_1 \to A_2} = \frac{H}{2}\left(\frac{H^2 + R_2^2 + 1}{\sqrt{(H^2 + R_2^2 + 1)^2 - 4R_2^2}} - \frac{H^2 + R_1^2 + 1}{\sqrt{(H^2 + R_1^2 + 1)^2 - 4R_1^2}}\right) \quad \text{(A.9)}$$

This formula is valid only if $l > r_2$

Where:

$H = h/l$

$R_1 = r_1/l$

$R_2 = r_2/l$

l is the distance between the face and the ring centre

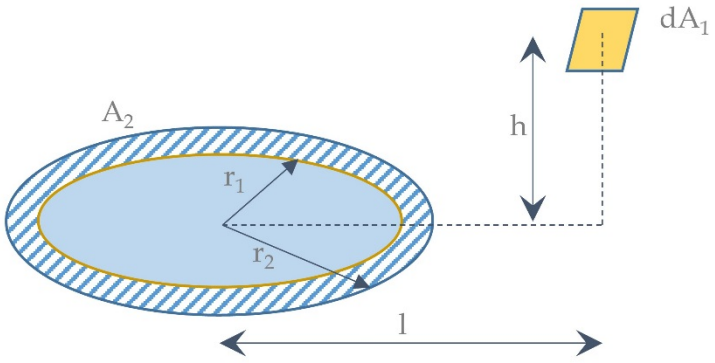

Figure A.11 Configuration ring – plane element

The annular part (ring z_i) between two cylinders is considered as a radiative surface (see Figure A.12) and the induced heat flux is computed from Equation (A.9). It is only added if $z_j > z_i$ (i.e. if the face "sees" the ring).

Additional rules need to be applied in order to cover all possible configurations using Equation (A.9). Theoretically, this equation is only valid for a ring centred in a plane perpendicular to the target, which is not always the case in practice (see Figure A.12)

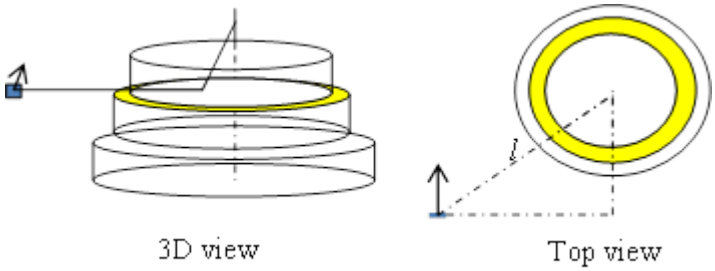

Figure A.12 Ring modelling (top view)

The orientation of the target has a strong impact on the heat flux exchanged between two surfaces (Figure A.13). Equation (A.9) corresponds to the case where the target is normal to the fire and gives the highest (most conservative) configuration factor.

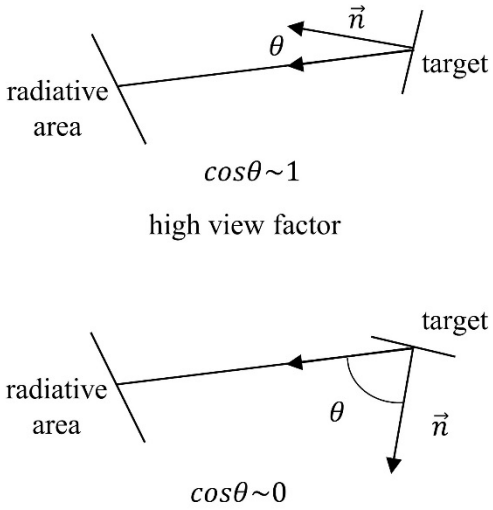

Figure A.13 Influence of the orientation of the target

It is also necessary to take into account the situation when the ring, as for the cylinder, is partially visible (see Figure A.14). In this case, the exterior and even the inner radius of the ring are reduced to give a visible ring using the same method applied to the cylinder. In the examples presented in the Figure, two cases are shown, for the ring defined by its inner radius r_{zi+1} and its outer radius r_{zi}. In case a, only the radius r_{zi} must be adjusted while in case b both r_{zi} and r_{zi+1} are adjusted.

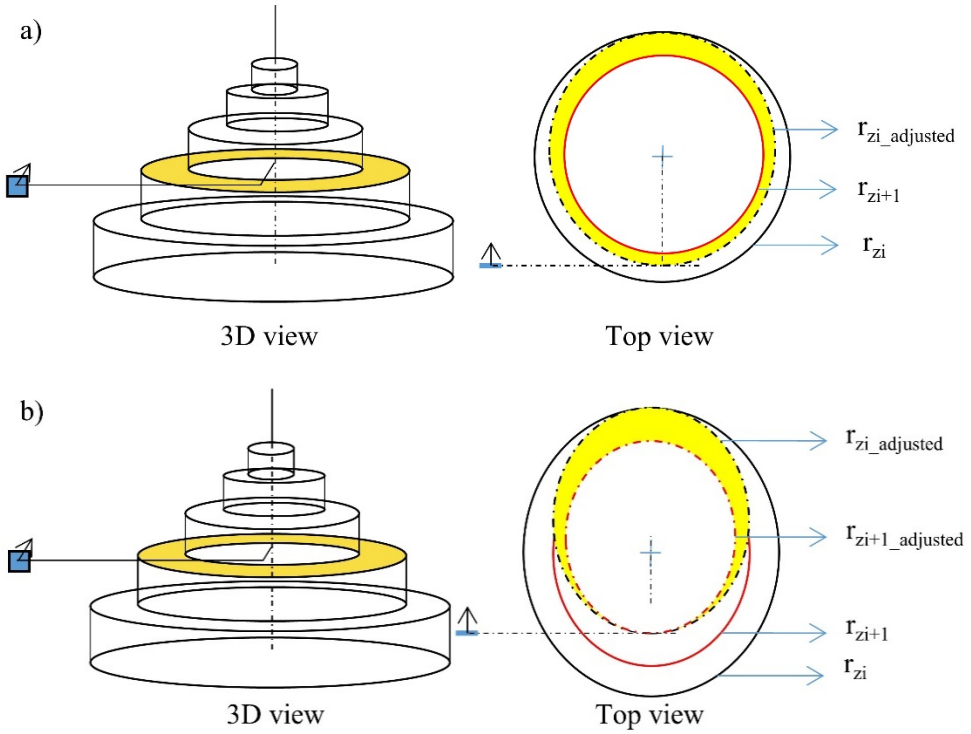

Figure A.14 Handling of complex case of ring modelling

The radiative heat flux received by a face is then the sum of the radiative heat flux emitted by all cylinders and rings:

$$\dot{h}_{solid\ flame \rightarrow face_j} = \sum_i \sigma.\varepsilon.\left(\theta_f(z_i) + 273\right)^4.\emptyset_{Cylinder\ z_i \rightarrow face_j} + \sum_i \sigma.\varepsilon.\left(\theta_f(z_i) + 273\right)^4.\emptyset_{Ring\ z_i \rightarrow face_j} \quad \text{(A.10)}$$

Finally, the mean radiative heat flux over the segment at the height z_j is computed by averaging the radiative heat flux over the four faces by the width l_i of each face:

$$\dot{h}_{rad,section\ z_j} = \frac{\sum_{i=1}^{4} l_i.\dot{h}_{solid\ flame \rightarrow face_i}}{\sum_{i=1}^{4} l_i} \quad \text{(A.11)}$$

A.2.1.4 Total heat flux received by a segment of the column

As stated previously, when the column is outside the flame and the considered segment is not in the smoke layer, then the total heat flux received is equal to the radiative heat flux:

$$\dot{h}_{total,section\ z_j} = \dot{h}_{rad,section\ z_j} \quad \text{(A.12)}$$

A.2.2 Column segment inside the smoke layer

In the smoke layer, the convective heat flux cannot be neglected. The smoke also has a strong impact on the radiative heat flux through absorption–emission phenomena, mainly by soot. The total heat flux received by a segment is calculated according to the following equations:

In a first step, the variable y is introduced:

$$y = \frac{d + H + z'}{L_h + H + z'} \tag{A.13}$$

Where:

d is the distance between the column and the centre of the fire area (Figure 4.2)

H is the distance between the fire source and the ceiling

If the fire origin is located at the height z_{fire} then:

$$H = h_{ceil} - z_{fire} \tag{A.14}$$

L_h is given by:

$$L_h = H\left(2.9Q_h^{0.33} - 1\right) \tag{A.15}$$

Q_h, a non-dimensional HRR, is estimated as:

$$Q_h = \frac{Q}{1.11\times10^6 H^{2.5}} \tag{A.16}$$

z' is defined by:

$$z' = 2.4D_{eq}\left(Q^{*2/5} - Q^{*2/3}\right) \qquad Q^* < 1 \tag{A.17}$$

$$z' = 2.4D_{eq}\left(1 - Q^{*2/5}\right) \qquad Q^* \geq 1 \tag{A.18}$$

Q^* is a non-dimensional HRR estimated in a similar way to Q_h:

$$Q^* = \frac{Q}{1.11\times10^6 D_{fire}^{2.5}} \tag{A.19}$$

The incident heat flux H_s is then calculated depending on the value of y:

$$\begin{cases} H_s = 100000 \text{ W/m}^2 & y \leq 0.3 \\ H_s = 136300 - 121000.y \text{ W/m}^2 & 0.3 < y < 1.0 \\ H_s = 15000.y^{-3.7} \text{ W/m}^2 & 1.0 \leq y \end{cases} \tag{A.20}$$

Finally, the total heat flux received by the segment z_j is:

$$\dot{h}_{section\, z_j} = H_s \tag{A.21}$$

A.3 Column inside the fire area

For a column inside the fire area, the convective heat flux is a major component of the total heat flux. In addition, the concept of solid flame where the external surface of the flame radiates towards a column is no longer correct.

EN 1991-1-2[2] gives a model to calculate the heat flux received at a point inside the fire. The model presented below is based on the Eurocode equations with a slight modification.

Again, a distinction is made between segments of the column which are not in the smoke layer under the ceiling and those which are.

A.3.1 Column segment outside the smoke layer

Column segments at the height z_j located between the ground and the height $(h_{ceil} - h_{smoke\ layer})$ are surrounded by hot gases at a temperature estimated from Equation (A.4). The incident heat flux is then calculated as:

$$\dot{h}_{inside\ flame} = \sigma.\varepsilon.\left(\left(\theta_f(z_j) + 273\right)^4 - 293^4\right) + \alpha_c\left(\theta_f(z_j) - 20\right) \qquad \text{(A.22)}$$

Where:

α_c is the coefficient of heat transfer by convection = 35 W/(m²K) in accordance with EN 1991-1-2

The total heat flux received by the segment z_j is then calculated as follows:

$$\dot{h}_{total,section\ z_j} = \dot{h}_{inside\ flame} \qquad \text{(A.23)}$$

A.3.2 Segment inside the smoke layer

For the segments of the column located in the smoke layer (between $(h_{ceil} - h_{smoke\ layer})$ and h_{ceil}), the total heat flux received is taken as the maximum between H_s calculated using the set of Equations (A.13) to (A.20) and $\dot{h}_{inside\ flame}$ calculated with Equation (A.22).

A.4 Total heat flux received by a segment of the column

The model presented in Section A.2 and A.3 assumes only one fire source. However, it is common to have fire scenarios where several sources are involved. In these cases, simple addition rules may be applied.

When the column is outside the fire area and not in the smoke layer, the radiative heat flux received by any face of the column is the sum of radiative heat fluxes emitted by each source assuming an upper limit of 100 kW/m^2.

If we consider n fire sources:

$$\dot{h}_{all\ solid\ flame \to face_j} = \min\left(100000,\ \sum_{i=1}^{n} \dot{h}_{solid\ flame_i \to face_j}\right) \qquad \text{(A.24)}$$

$$\dot{h}_{rad_{section}z_j} = \frac{\sum_{i=1}^{4} l_i . \dot{h}_{all\ solid\ flame \to face_i}}{\sum_{i=1}^{4} l_i} \qquad \text{(A.25)}$$

There is no change in the averaging procedure giving the total heat flux received by a column segment.

For all other cases, the total heat flux received is estimated by adding all heat fluxes of each fire source assuming again an upper limit of 100 kW/m².

ANNEX B APPLICATION TO A COLUMN OUTSIDE THE FIRE AREA

This annex gives an example which shows the practical application of the model. It should be noted that the techniques described in Section 4.2 allow the designer to determine the temperature rise in a column without the need for the complex numerical procedure outlined here.

B.1.1 Case description

The example is for a column outside the fire area and outside the smoke layer (this is the most complex case). Column segments inside the fire area or outside the fire area but inside the smoke layer present no special difficulties as the method uses classical and simple equations already in EN 1991-1-2.

Figure B.1 presents the general configuration assumed. The column is an HEB 300. It is located in front of a basin of diameter 4 m. The distance between the edge of the basin and the nearest face of the steel segment is 0.5 m. In the basin, a fuel is assumed to be burning at a constant rate of 1000 kW/m^2.

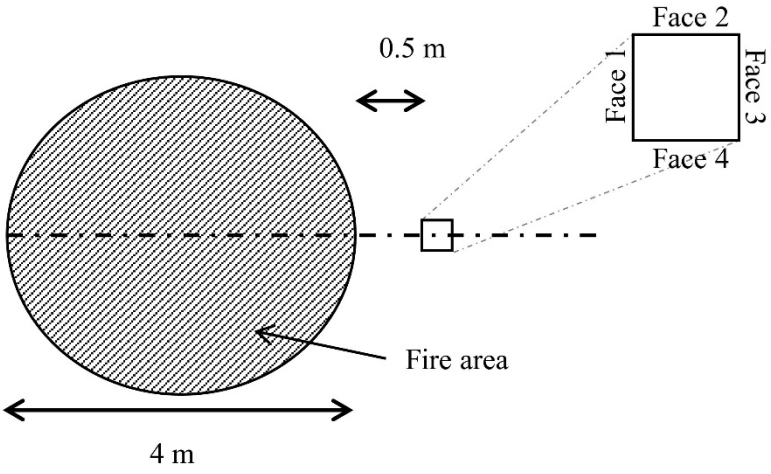

Figure B.1 Relative position of column and fire

B.1.2 Preliminary analysis

The calculation can be simplified in certain ways. The number of computations is proportional to the number of segments. Equation (A.6) is greatly simplified if segments are at heights which are a multiple of the cylinder height used to model the flame (0.5 m). In this case the variable y is equal to 0 (see Figure B.2) and Equation (A.6) reduces to:

$$\emptyset_{dA_1 \to A_2}(s,x,r,h) = \frac{S}{A} - \frac{S}{2A\pi}\{\pi + L_1 - L_2 + L_3\} \qquad \text{(B.1)}$$

$$L_1 = cos^{-1}\left(\frac{H^2 - A + 1}{H^2 + A - 1}\right)$$

$$L_2 = H\frac{H^2 + A + 1}{\sqrt{(H^2 + A - 1)^2 + 4H^2}}\ cos^{-1}\left(\frac{H^2 - A + 1}{\sqrt{A}(H^2 + A - 1)}\right)$$

$$L_3 = Hcos^{-1}\left(\frac{1}{\sqrt{A}}\right)$$

Where:

$$S = \frac{s}{r} \qquad X = \frac{x}{r} \qquad H = \frac{h}{r} \qquad A = X^2 + S^2 \qquad \text{(B.2)}$$

Consequently, calculations are carried out for segments at 0 m, 0.5 m, 1.0 m and so on. In the following paragraphs, the heat flux is calculated for a segment at 1.0 m height.

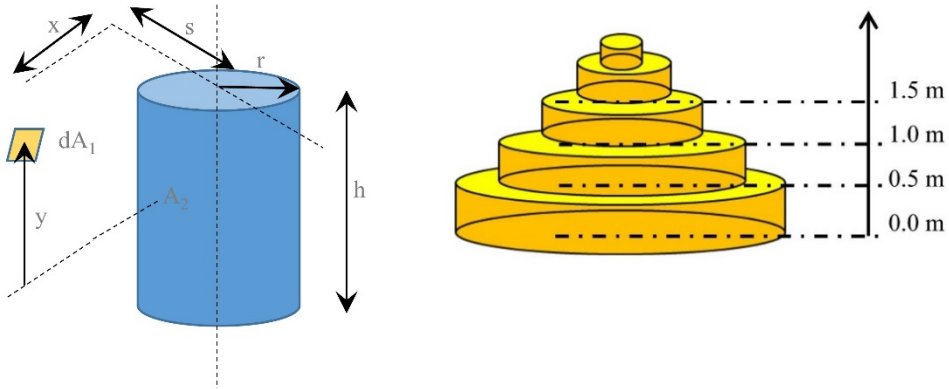

Figure B.2 Configuration cylinder-plane element (left) – height of segments for calculations (right)

Secondly, it is assumed that no radiative heat flux from the flame reaches face 3 with this configuration. Faces 2 and 4 are symmetric and will receive the same heat flux.

The final simplification concerns the position of the heat flux calculation for the faces. Although it should be done at the centre of each face, (see Figure B.3), as a simplification the computations are performed at the same position on the centre of Face 1. As it is the closest face to the basin, this will lead to the highest heat flux and is therefore conservative.

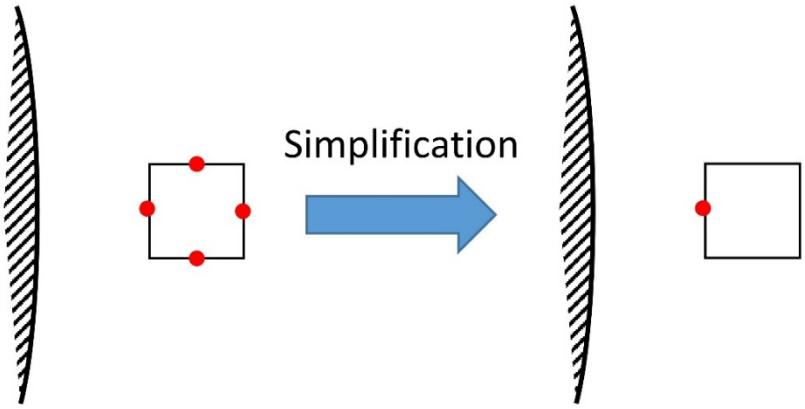

Figure B.3 Simplification for the position of each face for the heat flux calculation

B.1.3 Heat flux calculation

From Equations (A.2) to (A.5), it is possible to determine the properties of each cylinder and ring. In this case the flame height is 6.15 m (see Figure B.9). The heat flux received by each face is determined separately.

For Face 1, Equation (B.) can be used directly to compute the configuration factor between face 1 and the cylinders. Nevertheless, the rule of additivity must be used depending on the relative height between the cylinder and the face.

Considering the position depicted in Figure B.4 for Face 1 and a cylinder C_i (comprised between z_i and z_{i+1}), the position of the segment in the local coordinate system $(\vec{\imath},\vec{\jmath},\vec{k})$ can be taken as (s_f, x_f, z_f) which is (2.5, 0.0, 1.0). The four situations indicated in Figure B.5 can be encountered and must be decomposed as shown on the same figure.

If we define $\emptyset_i$ (respectively $\emptyset_{i+1}$), the configuration factor between Face 1 and a cylinder of height $|z_i - z_f|$ (respectively $|z_{i+1} - z_f|$) and radius r_i:

$$\begin{aligned}\emptyset_i &= \emptyset_{dA_1 \to A_2}\left(s = s_f, x = x_f, r = r_i, h = |z_i - z_f|\right)\\ \emptyset_{i+1} &= \emptyset_{dA_1 \to A_2}\left(s = s_f, x = x_f, r = r_i, h = |z_{i+1} - z_f|\right)\end{aligned} \tag{B.3}$$

Then the configuration factor $\emptyset$ between the Face 1 and the cylinder C_i is equal to:

$$\emptyset = |\emptyset_i - \emptyset_{i+1}| \tag{B.4}$$

The last part concerns the heat flux induced by rings. As the segment is at 1.0 m height, there is only one ring (at 0.5 m) below the segment. Using Equation (A.3), the radii (external and internal) of the ring can be calculated as follows:

$$\begin{aligned}r(z_i = 0.0) &= 2.00 \text{ m}\\ r(z_{i+1} = 0.5) &= 1.84 \text{ m}\end{aligned} \tag{B.5}$$

The incident heat flux is finally calculated by summing all contributions (Equation (A.9)). It leads to an incident heat on Face 1 of 76.36 kW/m² and, assuming an emissivity of 0.7, to an absorbed heat flux of 53.45 kW/m².

Figure B.9 shows this procedure implemented in an excel spreadsheet for this example.

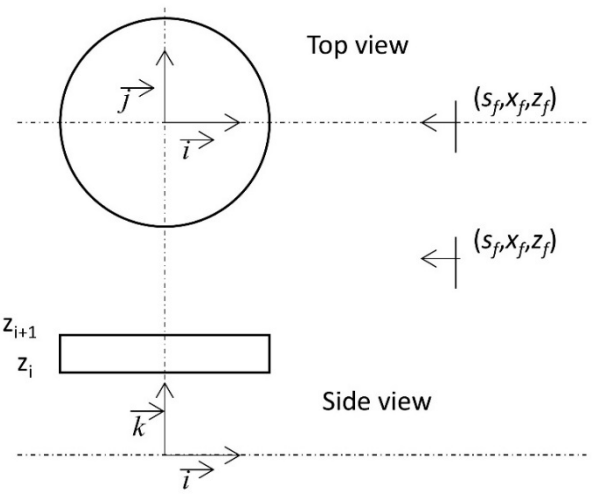

Figure B.4 Coordinates of face 1

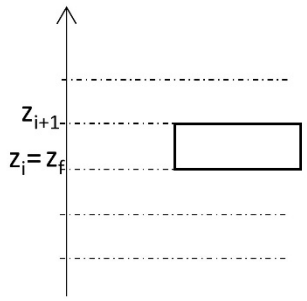

Figure B.5 Relative position face 1: cylinder and decomposition, Case a

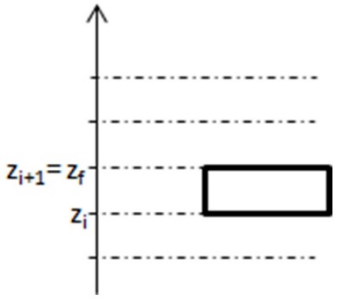

Figure B.6 Relative position face 1:– cylinder and decomposition, Case b

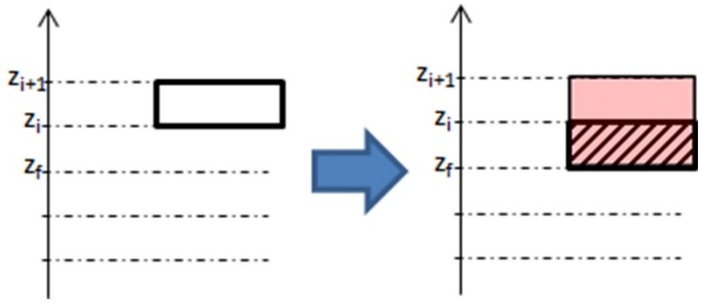

Figure B.7 Relative position face 1: cylinder and decomposition, Case c

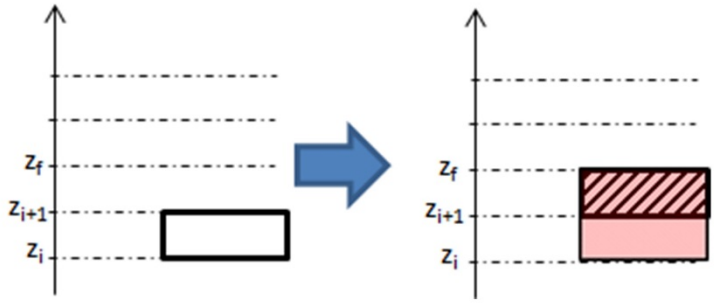

Figure B.8 Relative position face 1: cylinder and decomposition, Case d